DMD Fast Forward. Published on June 6, 2017 as DOI: 10.1124/dmd.117.075192
This article has not been copyedited and formatted. The final version may differ from this version.

DMD#75192

Title

Development of A Novel Maternal-Fetal Physiologically Based Pharmacokinetic Model I: Insights into Factors that Determine Fetal Drug Exposure through Simulations and Sensitivity Analyses

Zufei Zhang, Marjorie Z. Imperial, Gabriela I. Patilea-Vrana, Janak Wedagedera, Lu Gaohua and Jashvant D. Unadkat

Department of Pharmaceutics, University of Washington, Seattle, WA (ZZ, MI, GP, and JU); Simcyp Limited (a Certara company), Sheffield, UK (JW and LG)

Merck Sharp & Dohme Corp., Kenilworth, New Jersey, USA (ZZ, current affiliation) University of California San Francisco, Department of Bioengineering and Therapeutic Sciences (MI, current affiliation)

DMD Fast Forward. Published on June 6, 2017 as DOI: 10.1124/dmd.117.075192
This article has not been copyedited and formatted. The final version may differ from this version.

DMD#75192

Running Title: A PBPK model to elucidate factors determining fetal drug exposure

Corresponding Author:

Dr. Jashvant D. Unadkat

Department of Pharmaceutics

University of Washington

Box 357610

Seattle, WA 98195

Telephone: 206-543-9434

Fax: 206-543-3204

E-mail: jash@u.washington.edu

Number of words in the Abstract: 248

Number of words in the Introduction: 521

Number of words in the Discussion: 2112

Number of text pages: 25

Number of tables: 5

Number of figures: 9

Number of references: 79

DMD Fast Forward. Published on June 6, 2017 as DOI: 10.1124/dmd.117.075192
This article has not been copyedited and formatted. The final version may differ from this version.

Abbreviations:

ADMET: absorption, distribution, metabolism, excretion, and transport; AUC, area under the curve; BCS: biopharmaceutics classification system; B/P: blood to plasma concentration ratio; C_{max}: maximum plasma concentration; CL: clearance; CL_{f0}: fetal metabolic clearance; CL_{MP}: placental apical uptake clearance; CL_{m0}: maternal systemic clearance; CL_{p0}: placental metabolic clearance; CL_{PM}: placental apical efflux clearance; CL_{PD}: transplacental passive diffusion clearance; $CL_{PD,u}$: unbound transplacental passive diffusion clearance; CL_r: renal clearance; $CL_{int,u,hep}$: unbound hepatic intrinsic clearance; C-T: concentration-time ; CYP: cytochrome P450; $f_{m,\ CYP}$: fraction metabolized by a given CYP enzyme; $f_{u,p}$: fraction unbound in plasma; F: bioavailability; F_a: fraction absorbed; F_g: intestinal bioavailability; F_h: hepatic bioavailability; GA: gestational age; IV: intravenous; k_a: first order absorption rate constant; MP: maternal plasma; PBPK model: physiologically-based pharmacokinetic model; PK: pharmacokinetics; steady-state$_{inf}$: steady-state after an intravenous infusion; $t_{1/2}$: half-life; UV: umbilical vein; V_{ss}: volume of distribution at steady-state

Abstract

Determining fetal drug exposure (except at the time of birth) is not possible for both logistical and ethical reasons. Therefore, we developed a novel maternal-fetal physiologically based pharmacokinetic (m-f-PBPK) model to predict fetal exposure to drugs and populated this model with gestational age-dependent changes in maternal-fetal physiology. Then, we used this m-f-PBPK to: (1) perform a series of sensitivity analyses to **quantitatively** demonstrate the impact of fetoplacental metabolism and placental transport on fetal drug exposure for various drug dosing regimens administered to the mother; (2) predict the impact of gestational age on fetal drug exposure; and (3) demonstrate that a single umbilical venous: maternal plasma (UV:MP) ratio (even after multiple oral dose administration to steady-state) does not necessarily reflect fetal drug exposure. In addition, we verified the implementation of this m-f-PBPK model by comparing the predicted UV:MP and fetal:maternal plasma AUC ratios with those predicted at steady-state after an IV infusion. Our simulations yielded novel insights on the quantitative contribution of fetoplacental metabolism and/or placental transport on gestational-age dependent fetal drug exposure. Through sensitivity analyses, we demonstrated that the UV:MP ratio does not measure the extent of fetal drug exposure unless obtained at steady-state after an IV infusion or when there is little or no fluctuation in maternal plasma drug concentrations after multiple dose oral administration. The proposed m-f-PBPK model can be used to predict fetal exposure to drugs across gestational ages and therefore provide the necessary information to assess the risk of drug toxicity to the fetus.

DMD Fast Forward. Published on June 6, 2017 as DOI: 10.1124/dmd.117.075192
This article has not been copyedited and formatted. The final version may differ from this version.

Introduction

Fetal exposure to drugs has become increasingly common. This can be attributed to the rising use of therapeutic drugs among pregnant women (Mitchell et al., 2011) as pre-existing maternal conditions (e.g. epilepsy, asthma) or conditions developed during pregnancy (e.g. gestational diabetes and hypertension) must be treated to ensure the health and welfare of the mother and therefore her fetus. Sometimes, it is the unborn child that is the target of the treatment (e.g. to prevent maternal-fetal HIV transmission (McGowan and Shah, 2000)). Consequently, the ability to **quantitatively** evaluate fetal exposure to drugs and risk of toxicity, not only at term but also earlier during pregnancy when the fetus is most vulnerable to teratogens, is needed.

Unlike the general population, fetal exposure to drugs ingested by the pregnant mother cannot be readily studied prior to birth for ethical and logistical reasons. Even at the time of birth, assessment of fetal exposure to drugs is limited to a single cord plasma concentration measurement and reported as the umbilical vein: maternal plasma drug concentration ratio (UV:MP ratio). As shown here, in most clinical scenarios, this UV:MP ratio does not reflect the extent of fetal drug exposure relative to that in the mother. Nor does this ratio provide information on fetal drug exposure over time [i.e. fetal plasma AUC (AUC_f)] or maximum fetal plasma drug concentration ($C_{max,f}$) that often drives drug efficacy and/or toxicity in the fetus. Further, since cord blood sampling is limited to term, fetal drug exposure during early gestation remains unknown. To overcome these gaps in knowledge, mechanistic understanding of the determinants of fetal drug exposure and non-invasive approaches to predict fetal exposure across gestational ages, such as **P**hysiologically-**b**ased **P**harmaco**k**inetic (PBPK) modelling and simulation, are needed.

DMD Fast Forward. Published on June 6, 2017 as DOI: 10.1124/dmd.117.075192
This article has not been copyedited and formatted. The final version may differ from this version.

While a number of attempts to develop fetal PBPK models have been made (Clewell et al., 2007; Loccisano et al., 2013; Yoon et al., 2011), upon closer examination, except for a recently published model (De Sousa Mendes et al., 2015; De Sousa Mendes et al., 2016), the majority of these models are not intended to predict fetal exposure to therapeutic agents prescribed to pregnant women. Their limitations include: (1) incomplete inclusion of pregnancy-caused changes in maternal and fetal physiology; (2) not accounting for the alterations in maternal drug disposition; and (3) exclusion of fetal body compartments important for disposition of therapeutic drugs. Recently, our lab has successfully refined and verified a mechanistic maternal pregnancy PBPK model (m-PBPK) that can predict the maternal disposition of drugs cleared by one or more CYP enzymes during pregnancy (Ke et al., 2012, 2013b, 2014). However, this model only contains a lumped tissue compartment representing the placenta and fetus. Therefore, the goals of the current investigation were to: (1) develop a maternal-fetal PBPK (m-f-PBPK) model by incorporating a physiologically relevant fetal-PBPK into our previously verified m-PBPK; (2) **quantitatively** demonstrate the impact of fetoplacental metabolism and placental transport on fetal drug exposure; (3) **quantitatively** predict the impact of gestational age on fetal drug exposure; and (4) show that the UV:MP ratio after a single dose or after multiple dosing (even at steady-state) does not necessarily represent the extent of fetal drug exposure.

Materials and Methods

Model structure and general assumptions

Briefly, a m-f-PBPK model was built using MATLAB® (R2014b, Mathworks, Natick, MA) by adding the placenta, the amniotic fluid compartment, and fetal organs important in drug disposition (e.g. liver and kidney) and distribution (e.g. brain) (**Figure 1**) to our verified m-

PBPK model (Ke et al., 2013a; Ke et al., 2012, 2013b). The remaining fetal organs were lumped into a single compartment referred to as "rest of body". Our model also accounted for the marked differences in fetal circulation compared to that in the mother (Polin et al., 2004). For instance, it is the venous blood that carries oxygenated blood (via the umbilical vein) from the placenta to the fetus. The majority of this flow bypasses the fetal liver through the ductus venosus before perfusing fetal tissues.

General model assumptions include:

- The bidirectional unbound maternal-placental and fetal-placental transplacental passive diffusion clearances ($CL_{PD,u}$) across the placenta are equal and always present.
- For a given drug, the magnitude of $CL_{PD,u}$ is directly proportional to the placenta villous surface area which increases with gestational age.
- The UV plasma drug concentration represents the systemic fetal plasma venous drug concentration.
- Fetal renal clearance is negligible during the first 20 weeks of gestation (Polin et al., 2004). After week 20, it consists of only glomerular filtration clearance which can be estimated from fetal plasma protein binding and inulin clearance estimated in preterm (week 23 - 40) and term neonates (within first 14 days of life).
- Compared with fetal swallowing, the movement of amniotic fluid between the amniotic sac and maternal circulation is negligible (Gilbert and Brace, 1993). Therefore, fluid transfer between these two compartments was considered to be zero.

DMD Fast Forward. Published on June 6, 2017 as DOI: 10.1124/dmd.117.075192
This article has not been copyedited and formatted. The final version may differ from this version.

Collection and analyses of fetal physiological parameters

To populate the m-f-PBPK model with fetal physiological parameters, a systematic literature search was carried out using PUBMED to obtain these parameters (**Table 1)**. The search strategy was aimed to identify cohort studies whereby the parameter(s) of interest was longitudinally examined during gestation. Data from the control arm of case-control studies and healthy subjects of cross-sectional studies were considered for inclusion. Other inclusion criteria included: (1) human; (2) uncomplicated singleton pregnancies; (3) otherwise uneventful pregnancies with condition(s) thought not to affect the parameter of interest (e.g. preterm birth data were used to estimate fetal renal function). If the data were not tabulated and only graphs were present, individual data points were digitized using Digitizer (a free MATLAB® tool available on http://www.mathworks.com/matlabcentral/). When multiple qualified studies were available for a physiological parameter of interest, data were pooled, stratified by gestational age (measured in weeks from the first day of the last menstrual cycle) and summarized using the approach previously published (Abduljalil et al., 2012). For a given GA, the overall sample size weighted mean parameter value $\overline{X}$ from different studies was calculated as follows: $\overline{X} = \frac{\sum_{i=1}^{i} n_i X_i}{\sum_{i=1}^{i} n_i}$,

where n_i is the number of subjects in the ith study and X_i is the mean value from that study. In cases whereby both mean values and variability (SD or SE) of various GA groups were provided, overall SD was calculated as $\overline{SD} = \sqrt{\frac{\sum_{i=1}^{i}[(SD_i)^2 + (X_i)^2] \cdot n_i - N \cdot \overline{X}^2}{N}}$ where SD_i is the standard deviation in the ith study and, n_i is the number of subjects in the ith study, and X_i is the mean

value from that study. When individual measurements associated with a given GA were not available, the average values computed from formulae across publications were used instead.

Data analysis was performed using Excel (2010, Microsoft®, Redmond, WA). In general, polynomial, exponential, or power function equations were chosen to describe the longitudinal changes in parameters during development. The choice of the polynomial degree was determined by fitting various polynomials to data using nonlinear regression. If a higher order of polynomial equation did not reduce R^2 value and/or if it departed from the original data in comparison with a lower degree by visual check, then the lower one was chosen. Exponential and power equations were chosen to describe parameters when polynomials did not adequately fit rapidly time-varying parameters.

Sensitivity analyses to identify key determinants of fetal drug exposure

To identify the quantitative impact of key factors (e.g. fetal metabolic clearance) that influence maternal-placental/fetal plasma concentration-time (C-T) profiles of a drug at term (week 40), we conducted a series of simulations of two hypothetical drugs, X and Y (**Table 2**), using our newly developed m-f-PBPK model. Drug X was designed to be a neutral compound (such as the HIV nucleoside drugs zidovudine and didanosine which are predominately unionized at physiological pH) with intermediate permeability across the placenta and minimal plasma protein binding. Therefore, all the variables and parameters discussed here for drug X should be read as unbound values. A drug of these characteristics was chosen to quantitatively illustrate the impact of fetoplacental metabolism and placental transport on fetal exposure to drugs. Drug Y was designed to represent highly lipophilic, neutral drugs with high permeability across biological membrane. It was significantly bound to plasma albumin. Consequently, its

DMD Fast Forward. Published on June 6, 2017 as DOI: 10.1124/dmd.117.075192
This article has not been copyedited and formatted. The final version may differ from this version.

maternal-fetal distributional equilibrium was affected by differences in maternal vs. fetal plasma albumin concentrations. Relevant examples include protease inhibitors and many BCS class I and II drugs. These drugs are cleared by P450 enzymes that have altered activity during pregnancy (Isoherranen and Thummel, 2013).

Additional assumptions made for the hypothetical drugs X and Y are as follows:

- Drug X is neutral, follows linear kinetics, and has negligible binding in the maternal and fetal plasma and in the placenta. Therefore, all concentrations and clearances of drug X represent their corresponding unbound values.
- Drug Y is neutral, exhibits linear kinetics, and binds to plasma albumin. Its binding in the placenta tissue is the same as that in the maternal plasma.
- Maternal absorption of drug X or Y is first order and does not change during pregnancy [i.e. absorption rate constant (k_a), fraction absorbed (F_a), and fraction escaping gut metabolism (F_g)].
- Maternal and fetal tissue-to-plasma partition coefficients (K_p's) are identical for both drugs and remain constant throughout pregnancy.
- Except where indicated, fetal renal clearance of drug X or Y is negligible.
- Drug X or Y swallowed by the fetus (i.e. the amniotic fluid) is instantly and completely absorbed from the fetal intestine and is not metabolized there.

While some of the above assumptions were made to simplify the simulations (e.g. neutrality thus zero ionization; unaltered maternal absorption during pregnancy), others were made (e.g. fetal renal secretion of drugs) because these values cannot be determined.

Except where indicated, the simulations were conducted using our m-f-PBPK model where only one parameter was changed at a time (**Tables 3** and **4**) at week 40.

Effect of gestational age on the fetal-maternal plasma pharmacokinetics

We simulated the impact of gestational age on exposure of the maternal-fetal unit to drug X or Y under various scenarios (**Table 5**). Week 20 and week 40 were chosen, respectively, to represent the gestational age when fetal skin keratinization begins and when cord blood sampling is possible. Fetal metabolic clearance of drug X, when present, was assumed to be directly proportional to fetal body volume as the metabolism of HIV nucleoside drugs (i.e. phosphorylation) occurs throughout the body. Where invoked, placental efflux clearance (CL_{PM}) was assumed to be mediated by P-gp, and the magnitude of this clearance was assumed to be proportional to the expression of P-gp in the placenta. At term, P-gp mediated CL_{PM} was arbitrarily set at 20% of CL_{PD}. In the absence of placental P-gp expression data at week 20, we assumed that placental P-gp expression decreases by 5-fold based on our first trimester data on placental P-gp expression (Mathias et al., 2005). This change in expression was then scaled up to the whole placenta based on change in the gestational age-dependent placental volume (Abduljalil et al., 2012).

Results

Fetal physiological parameters

The time-variant fetal physiological parameters used to populate the m-f-PBPK model show that the gestational age-dependent changes in fetal physiological parameters are pronounced (**Table 1**). For example, umbilical venous blood flow (i.e. fetal placental blood flow) increases by

DMD Fast Forward. Published on June 6, 2017 as DOI: 10.1124/dmd.117.075192
This article has not been copyedited and formatted. The final version may differ from this version.

approximately 6.2-fold (from 3.3 L/h to 20.2 L/h) from week 20 to week 40. Some fetal physiological values change with gestational age in an opposite direction to the corresponding values in the mother. For example, the fetal plasma albumin concentrations increase with gestational age while the reverse is true for the mother.

Impact of maternal metabolism and placental passive drug permeability on fetal exposure to Drug X or Y in the absence of placental/fetal metabolism or placental transport

As expected, after continuous intravenous (IV) infusion of drug X or Y, both steady-state (steady-state$_{inf}$) maternal venous plasma (MP) and fetal venous plasma (fetal plasma) concentrations and the time to reach steady-state$_{inf}$ were inversely dependent on the maternal drug clearance (CL_{m0}) when V_{ss} was held constant (**Figure 2a**,**2b**,**3a**,**3b**). In contrast, for both drugs, maternal plasma C-T profile, but not the fetal plasma C-T profile, was independent of the transplacental passive diffusion clearance of the drug (CL_{PD}) as were the maternal and fetal steady-state$_{inf}$ plasma concentrations (**Figure 4a**,**5a**). Although total fetal plasma steady-state$_{inf}$ concentrations of drug Y were consistently higher than those in the mother (**Figure 3a**,**3b**,**5a**,**5b**), for both drugs, the corresponding unbound steady-state$_{inf}$ UV:MP ratio remained unity irrespective of the magnitude of CL_{m0} or CL_{PD} (**Figure 2b**,**4b** for drug X; data not shown for drug Y). However, for both drugs, the time to reach fetal steady-state$_{inf}$ plasma concentration was prolonged with lower CL_{m0} or CL_{PD} (**Figure 2b**,**3b**,**4b**,**5b**). Of note, the simulated UV:MP ratio of drug X which is not bound to plasma proteins) or Y (after correcting for plasma protein binding) matched those predicted by our steady-state$_{inf}$ model (see **Supplementary Information**).

DMD Fast Forward. Published on June 6, 2017 as DOI: 10.1124/dmd.117.075192
This article has not been copyedited and formatted. The final version may differ from this version.

Following a single oral dose of drug X or Y, fetal drug exposure [fetal plasma AUC (AUC_f)] was inversely proportional to CL_{m0} (**Figure 2c**, **3c**) but independent of CL_{PD} (**Figure 4c, 5c**) though the fetal plasma t_{max} ($t_{max,f}$) and $C_{max,f}$ were affected by both clearances. As expected, their UV:MP ratios varied over time until maternal-fetal distributional equilibrium was achieved (**Figure 2d**,**3d**,**4d**,**5d**). Interestingly, for both drugs (but drug X more than drug Y), its distributional equilibrium UV:MP ratio was greater than the expected value of unity in the absence of fetoplacental metabolism or drug transport (**Supplementary Eq.1**). For drug Y, this deviation from unity persisted after correcting for plasma protein binding (data not shown). Furthermore, for both drugs, the deviation from unity became significantly dampened with decrease in CL_{m0} (**Figure 2d**,**3d**) or increase in CL_{PD} (**Figure 4d**,**5d**).

After multiple oral doses, as expected, the time to reach steady-state, and the accumulation and fluctuations in steady-state maternal plasma drug concentrations was inversely proportional to CL_{m0} (**Figure 2e**,**2g**,**3e**,**3g**), but independent of changes in CL_{PD} (**Figure 4e**,**5e**). However, higher CL_{PD} resulted in greater fluctuations in steady-state fetal plasma drug concentrations within a dosing interval (**Figure 4e**,**5e**). Overall, the effect of CL_{m0} or CL_{PD} on the UV:MP ratio remained the same after single or multiple oral dosing.

Impact of dosing interval (τ) on UV:MP ratio of drug X or Y in the absence of placental/fetal metabolism or placental transport

As expected, shortening τ resulted in greater drug accumulation (**Figure 2e** vs **2g**, **Figure 3e** vs **3g**) but less fluctuations in the UV:MP ratio within a dosing interval (**Figure 2f** vs **2h**, **Figure 3f** vs **3h**). Like in the above scenarios, the observed distributional equilibrium UV:MP ratio of drug

DMD Fast Forward. Published on June 6, 2017 as DOI: 10.1124/dmd.117.075192
This article has not been copyedited and formatted. The final version may differ from this version.

X and Y remained higher than the expected unbound steady-state$_{inf}$ UV:MP ratio of 1.0 and the extent of this deviation was inversely related to CL_{m0} (**Figure 2f**, **2h**, **3f**, **3h**).

Impact of placental drug transport, fetal metabolism, and placental metabolism on fetal exposure to drug X or Y

Overall, variations in these pathways (**Table 3**) produced significant changes in fetal plasma C-T profiles of drug X without affecting maternal pharmacokinetics (PK) (data not shown). As expected, following a single oral dose of 400 mg drug X , fetal plasma concentrations, fetal plasma C_{max} ($C_{max,f}$), and placental concentrations (not shown) of drug X were inversely correlated with its metabolism in the placenta (CL_{p0}) (**Figure 6a1**), in the fetus (CL_{f0}) (**Figure 6b1**), or both (**Figure 6c1**). Irrespective of the magnitude of CL_{p0} relative to CL_{PD}, the effect of change in CL_{p0} on the magnitude of reduction in AUC_f and placental AUC (AUC_p) were identical (**Figure 6a2**). In contrast, an increase of the same magnitude in fetal metabolism (CL_{f0}) resulted in a greater reduction in AUC_f compared to AUC_p (**Figure 6b2**). For example, when CL_{p0} equaled CL_{PD}, AUC_p and AUC_f were both reduced by 50%, whereas when CL_{f0} equaled $CL_{PD,}$ a greater reduction in AUC_f was seen compared with AUC_p (67% vs. 33%) (**Figure 6a2**vs **6b2**). When both metabolic processes were present (CL_{p0} and CL_{f0}) and equal to CL_{PD}, the reduction in the $C_{max,f}$ (**Figure 6c1**), AUC_p (60%), and AUC_f (80%) was even greater (**Figure 6c2**). The addition of uptake (CL_{MP}) or efflux (CL_{PM}) clearance on the apical side of the placenta altered fetoplacental exposure to drug X in opposite directions (**Figure 6d** vs **6e**). While increasing CL_{MP} resulted in higher fetal plasma drug concentrations and $C_{max,f}$ (**Figure 6d1**) as well as increased F:M and placental:maternal (P:M) plasma AUC ratios (**Figure 6d2**), increasing CL_{PM} lowered $C_{max,f}$ (**Figure 6e1**) and reduced F:M and P:M plasma AUC ratios

DMD Fast Forward. Published on June 6, 2017 as DOI: 10.1124/dmd.117.075192
This article has not been copyedited and formatted. The final version may differ from this version.

(**Figure 6e2**). The predicted F:M and P:M plasma AUC ratios **quantitatively** matched those predicted by our steady-state$_{inf}$ model (**Supplementary Eq. 1** and **2**, respectively). However, even under fetal-maternal distributional equilibrium the UV:MP ratio (**Figure 6a3-6e3**) deviated from its respective steady-state$_{inf}$ F:M plasma drug concentration ratio and therefore did not represent F:M plasma AUC ratio.

Overall, following a single oral dose of drug Y, within the test range, variations in the same set of drug Y clearance pathways (**Table 4**) produced similar changes in fetal plasma drug concentrations (**Figure 7a1-e1**) without altering maternal plasma C-T curve of drug Y (data not shown). As was the case with drug X, both P:M and F:M AUC ratios decreased as these clearance pathways became larger with the exception of CL_{MP}, which was positively correlated with P:M and F:M ratios. After accounting for binding, the impact of fetal clearance was larger than that of placental clearance on F:M and P:M AUC ratios (**Figure 7a2-e2**). In addition, the predicted drug Y UV:MP ratio at distributional equilibrium (**Figure 7a3-e3**) was consistently higher than the expected steady-state$_{inf}$ UV:MP ratios (**Supplementary Eq. 1**).

Impact of gestational age on fetal disposition of drug X

Maternal and fetal plasma C-T profiles following a single 400mg oral dose of drug X at weeks 20 and 40 were simulated using the m-f-PBPK model under various scenarios outlined in **Table 3**. Gestational age significantly altered fetal plasma C-T profile while minimally affecting maternal PK (**Figure 8**). Furthermore, the impact of gestational age on fetal exposure to drug X depended on the clearance mechanisms within the fetoplacental unit. In scenario 1 (**Figure 8a, b**) where drug X was assumed to passively diffuse across the placenta without placental drug transport or irreversible clearance in the fetoplacental unit (e.g. metabolism), despite a modest 16%

DMD Fast Forward. Published on June 6, 2017 as DOI: 10.1124/dmd.117.075192
This article has not been copyedited and formatted. The final version may differ from this version.

decrease in $C_{max.f}$, the F:M plasma AUC ratio remained unity and did not change with advancing gestational age. In scenario 2 (**Figure 8c, d**), addition of fetal metabolism produced significant reduction in both the $C_{max,f}$ and AUC_f resulting in F:M plasma AUC ratio of 0.48 and 0.50 at week 20 and week 40, respectively. In Scenario 3 (**Figure 8e, f**) where P-gp mediated placental efflux clearance (CL_{PM}) was assumed to be 20% of CL_{PD} with no fetal metabolism, advancing gestation age from week 20 to week 40 and the associated decrease in CL_{PM} resulted in substantial changes in the shape of fetal C-T curve as well as in increase in $C_{max,f}$ (by 118.5%) and fetal AUC (by 3.6-fold). Finally, in Scenario 4 (**Figure 8g, h**), the combination of both fetal metabolism and placental efflux resulted in the lowest $C_{max,f}$ and AUC_f at both gestational ages.

Impact of gestational age on fetal disposition of drug Y

Overall, gestational age had a marked effect on maternal-fetal plasma C-T curves of drug Y. In scenario 1 where neither fetoplacental metabolism or placental drug transport was present and maternal hepatic unbound intrinsic clearance ($CL_{int,uhep}$) remained independent of gestational age, increasing gestational age resulted in slightly lower maternal plasma concentrations of drug Y (**Figure 9a**), as evidenced by a 19% reduction in maternal plasma AUC from week 20 to week 40. Over the same period, fetal plasma AUC increased significantly by 67% (**Figure 9b**). This decrease in ACU_m, in conjunction with the increase in AUC_f , resulted in a pronounced ~100% increase in F:M AUC ratio from week 20 to 40. However, after correcting for plasma protein binding, unbound F:M AUC ratios remained unity at both gestational ages (**Figure 9c**). In scenario 2 when a 100% induction in maternal $CL_{int,u,hep}$ at week 40 relative to that at week 20 was assumed, the resultant higher CL_{m0} gave rise to lower AUC_m and thus a 34% decrease in term AUC_f (**Figure 9d,e**) compared with scenario 1. Of note, F:M AUC ratios, both total and

DMD Fast Forward. Published on June 6, 2017 as DOI: 10.1124/dmd.117.075192
This article has not been copyedited and formatted. The final version may differ from this version.

unbound, were identical to those in Scenario 1(**Figure 9f**) with unbound F:M AUC ratios being unity. Like drug X, introduction of CL_{PM} (20% of CL_{PD} at term) in scenario 3 produced markedly lower fetal plasma drug concentrations and hence much smaller AUC_f at week 20 compared to week 40 (**Figure 9h**). Unbound F:M AUC ratios reduced to lower-than-unity values (~0.2 and ~ 0.8 at week 20 and 40, respectively)(**Figure 9i**). Lastly, in scenario 4, the combination of placental efflux and increasing CL_{m0} with gestational age resulted in pronounced difference in maternal-fetal plasma drug C-T curves between week 20 and week 40. Increase in CL_{m0} from week 20 to 40 in gestational age led to significantly lower maternal drug Y concentrations and a greater-than-50% reduction in AUC_m at week 40. When compared with Scenario 3, this scenario had much lower $C_{max,f}$ and AUC_f values at week 40 (**Figure 9j,k**), whereas the F:M AUC ratios were of the same magnitude (**Figure 9l**).

Discussion

Here we present a novel maternal-fetal PBPK model that, to our knowledge, allows for the first time the capability to predict fetal disposition of pharmaceutical drugs at various gestational ages. The model incorporated the unique fetal vascular physiology and allows future incorporation of placental transport and metabolism within the fetoplacental unit (in progress in our laboratory). This model has been verified by us, at term, where the predicted and observed maternal and fetal plasma concentrations of theophylline and zidovudine were in a good agreement (Zhang and Unadkat, 2017). However, since such verification data can only be collected at term and do not speak to which factors might affect this ratio (after a single or dose or at steady-state), we have used this novel m-f-PBPK model to **quantitatively** demonstrate the factors that can affect this ratio and when this ratio can and cannot be used to estimate fetal exposure to drugs (**Figures 2-9**).

DMD Fast Forward. Published on June 6, 2017 as DOI: 10.1124/dmd.117.075192
This article has not been copyedited and formatted. The final version may differ from this version.

While some of these results are obvious from fundamental pharmacokinetic principles, others are not. These unexpected results are highlighted below and summarized in **Supplementary Table 2.** Also, note that all fetoplacental clearance pathways below refer to clearance values after accounting for binding.

When does UV:MP ratio reflect fetal drug exposure?

Contrary to the widely held belief, the UV:MP ratio, even at distributional equilibrium, does not indicate fetal drug exposure relative to that in the mother (AUC_f/AUC_m) (**Figures 2-7**). The only exception is when the drug is administered to steady-state via an infusion or when maternal plasma concentrations, at steady-state, do not fluctuate much after multiple oral administration situations that occur infrequently in the clinic. The same UV:MP ratio is often deemed to infer the mechanisms by which the drug crosses the placenta. A greater than unity ratio is often interpreted as accumulation of the drug in the fetal compartment (Else et al., 2011). In contrast, a ratio of less than unity is interpreted as low fetal exposure and is attributed to low maternal drug concentrations (Chappuy et al., 2004a; Chappuy et al., 2004b), fetal metabolism (Ngan Kee et al., 2009), and/or placental efflux (Else et al., 2011; Marzolini and Kim, 2005). However, as shown by our simulations, such interpretations can be false. While fetal/placental metabolism or placental transport processes cannot be discounted based on a single UV:MP ratio, such deviation from unity is more likely due to the time-dependent distributional kinetics of the drugs across the placenta.

In the absence of fetal/placental metabolism or placental transport, the unbound steady-state$_{inf}$ UV:MP ratio and therefore the unbound F:M plasma AUC ratio after single or multiple doses

(assuming linearity) should be unity (**Supplementary Eq. 1**). Indeed it is (**Figures 2-7**). In all other cases, the degree of deviation of this ratio from unity (sometimes by an order of magnitude) not only varied with time but also depended on the magnitude of transplacental passive diffusion clearance (CL_{PD}, **Figures 4** and **5**) and maternal clearance (CL_{m0}, **Figures 2** and **3**). The extent of this deviation decreased when the fetal compartment was allowed to rapidly equilibrate with the maternal compartment. Even in these cases where no active placental uptake was invoked, the UV:MP ratio at distributional equilibrium still exceeded unity (~1.7 and 1.5 in **Figure 2d** and **3d**, respectively). While puzzling at first glance, these observations can be explained by the multi-compartmental PK of drugs X and Y. During the post-distributive phase, the peripheral:central compartment drug concentration ratio increases as the central compartment clearance is increased or as the inter-compartmental clearance is decreased (see **Supplementary Information** for details). The above conclusions also hold true for multiple dosing regimens (**Figures 2-5**). Our simulations are consistent with literature reports. For example, after the last maternal dose, the UV:MP ratio of zidovudine ($t_{1/2}$ ~ 1.1 h)(Collins and Unadkat, 1989) range from 0.18 to 17.2 (Chappuy et al., 2004a), whereas that of theophylline ($t_{1/2}$ ~ 8h) is much less variable (from 0.98 to 1.59) (Ron et al., 1984). Clearly, in the case of zidovudine, interpreting UV:MP ratios of much greater than 1.0 as indicative of active maternal-fetal transport would be incorrect. Similarly, another frequently reported ratio, the amniotic fluid:UV drug concentration ratio, varied with time and did not reflect fetal drug exposure (see **Supplementary information**).

Unbound F:M AUC ratio is determined by the magnitude of placental clearance relative to fetoplacental and/or placental transport clearance

DMD Fast Forward. Published on June 6, 2017 as DOI: 10.1124/dmd.117.075192
This article has not been copyedited and formatted. The final version may differ from this version.

Another common misconception about fetal drug exposure (i.e. AUC_f) is that AUC_f is mainly driven by maternal plasma drug concentrations and not by passive placental transfer and/or fetoplacental metabolism. The reasoning behind it is that fetal/placental clearances are thought to be minor compared to maternal clearance of the drug, due to the small size of the fetal liver [only about 9.5% of maternal liver weight at term (Abduljalil et al., 2012)] or the limited metabolic capacities of the placenta and the fetal liver. Therefore, it is often assumed that when active transport across the placenta is absent, the unbound F:M AUC ratio will approximate unity. While maternal plasma drug concentrations do drive fetal plasma drug concentrations, the above reasoning about F:M AUC ratio is false because it fails to recognize an additional critical factor, CL_{PD}. It is the ratio of these two clearances (i.e. the magnitude of fetoplacental clearance(s) relative to CL_{PD} and not relative to CL_{m0}) that determines the unbound F:M AUC ratio. These determinants of fetal drug exposure, however, have been largely overlooked by others (Bernick and Kane, 2012; Hill and Abramson, 1988; Marzolini and Kim, 2005; Myllynen et al., 2007) and are discussed below with examples (**Figures 6** and **7**).

For relative polar drugs with intermediate or low CL_{PD} (e.g. drug X), introduction of fetal/placental metabolism and/or placental transport can significantly alter fetal drug exposure if their magnitude is significant relative to CL_{PD} (**Figure 6**). It is important to stress here that the reference point is CL_{PD} and not CL_{mo}. Consistent with our simulations, due to fetal metabolism, the unbound steady-$state_{inf}$ F:M plasma drug concentration ratios of two predominantly polar dideoxynucleoside HIV drugs, didanosine and zalcitabine, were , 0.48 and 0.63 in the chronically catheterized maternal-fetal macaques (Pereira et al., 1994; Tuntland et al., 1996). Furthermore, our simulations yielded another novel insight. The site of drug clearance (placental, fetal, or

DMD Fast Forward. Published on June 6, 2017 as DOI: 10.1124/dmd.117.075192
This article has not been copyedited and formatted. The final version may differ from this version.

both) had differential impact on AUC_f and AUC_p (**Supplementary Eq.1**, **Eq. 2**, and **Figure 6**). Because any drug taken by mother has to first traverse the placenta to reach fetal circulation, the placenta essentially behaves like the "fetal gut". If metabolism or drug efflux/influx occurs only in the placenta, then the change in placental and fetal drug exposure will be identical and will depend on the degree of pre-systemic "first pass"(**Figure 6a, 6d,6e**). Instead, if metabolism (of equal magnitude) occurs in the fetus, this will result in a greater reduction in AUC_f compared to AUC_p (**Figure 6b, 6c**). In essence, metabolism in the fetus magnifies the reduction in fetal drug exposure caused by placental clearance. This "site effect" may have clinical implications as fetal toxicity can occur via toxicity to the placenta (e.g. formaldehyde) (Pidoux et al., 2015). In these cases, fetal toxicity cannot be readily ruled out even when fetal exposure to the toxin/drug is low. In contrast, when CL_{PD} of drugs is much greater than fetal/placental metabolism or placental transport (e.g. lipophilic drugs such as drug Y), the placenta becomes "transparent". In other words, fetal and maternal compartments rapidly equilibrate. Therefore, AUC_f will approach or equal AUC_m after single dose or multiple dose administration of the drug (assuming linearity) (**Figure 7b).** In reality, for lipophilic drugs with limited fetoplacental metabolic capacities, negligible effect on AUC_f is expected when CL_{f0} or CL_{p0} are varied. However, even for such drugs, in the presence of significant fetal/placental metabolism and/or placental transport relative to CL_{PD}, fetal drug exposure will be significantly altered (e.g. remifentanil(Coonen et al., 2010; Egan, 1995)). Several lipophilic HIV protease inhibitors that are P-gp substrates (e.g. ndinavir, ritonavir, and saquinavir) (Unadkat et al., 2004) haveUV:MP ratios that are considerably lower than unity (Marzolini and Kim, 2005). However, as pointed out earlier, these non-steady-state$_{inf}$ ratios should be interpreted with caution. Nevertheless, a role of placental P-gp efflux likely

contributes to their low fetal exposure as these drugs are excellent substrates of P-gp (McCormack and Best, 2014)(van der Sandt et al., 2001).

The impact of gestational age on fetal drug exposure

The expression of fetoplacental drug metabolizing enzymes (DMEs) and placental transporters are known to change with gestational age (Myllynen et al., 2009). For this reason, fetal drug exposure (with no change in maternal dosage regimen) is likely to change with gestational age (**Figures 8** and **9**). But these changes are not intuitive. When drug X passively diffused across the placenta without being transported or metabolized in the fetoplacental unit (**Figure 8a, 8b**), progression of gestation did not affect AUC_f because the latter was solely driven by AUC_m, which remained virtually the same from week 20 to week 40. In scenario 2, where only fetal metabolic clearance was present, AUC_f was significantly reduced and appeared nearly equal between week 20 and week 40 (**Figure 8d**). This is because the CL_{f0} /CL_{PD} ratio remained similar from week 20 to week 40 (0.53 and 0.50, respectively) due to the fact that fetal body volume (therefore fetal metabolic clearance) and the placental surface area (and therefore CL_{PD}) increased with gestational age in a nearly parallel fashion (**Table 1**). Placental P-gp expression is significantly higher during early gestation vs. term (Mathias et al., 2005). This gestational effect in P-gp expression resulted in lower fetal exposure to drug X at week 20, whereas at week 40, due to lower placental P-gp efflux clearance, fetal exposure to drug X increased by 1.9-fold (**Figure 8e, f**). When both clearance pathways were present, the change in placental P-gp expression was a major determinant of the gestational-age effect on drug X AUC_f (**Figure 8g, h**).

Challenges for the next generation of fetal PBPK models

DMD Fast Forward. Published on June 6, 2017 as DOI: 10.1124/dmd.117.075192
This article has not been copyedited and formatted. The final version may differ from this version.

Like other fetal PBPK models, our m-f-PBPK model also has some limitations. The use of our model to predict fetal exposure to drugs prior to week 20 may be limited for the following reasons. First, data on many fetal physiological parameters prior to week 20 (**Table 1**) are not available. Second, fetal skin is not completely keratinized and is highly permeable during the first half of gestation (Polin et al., 2004). Therefore, drugs that extensively partition into the skin/subcutaneous layer may readily cross into the amniotic fluid. Such movement of drugs could be incorporated into a future iteration of this model. In order for the model to be useful for drugs that are extensively metabolized by the fetus or transported/metabolized in the placenta, the model will need to be populated with gestational age dependent changes in the expression of these enzymes and transporters. Such studies, using quantitative targeted proteomics, are in progress in our laboratory.

Currently, lack of critical data hinders further development of fetal PBPK models. First, feto-placental physiological data across developmental stages are much needed, including the substantial changes in placental and fetal circulation and fetal organ sizes and composition. Obtaining such information will rely on the advancements in non-invasive physiological measurement techniques and devices. Before such information becomes available, cross-species extrapolation through PBPK modeling and simulation can be conducted (Poet et al., 2010; Yoon et al., 2011) . However, this approach will not work when there are significant interspecies differences in fetoplacental metabolism and placental transport. Another challenge lies in obtaining data for PBPK model validation. As detailed above, UV:MP ratio can change dramatically with time. Therefore, we propose that the maternal dosing regimen, the time post

DMD Fast Forward. Published on June 6, 2017 as DOI: 10.1124/dmd.117.075192
This article has not been copyedited and formatted. The final version may differ from this version.

last maternal dose when maternal and umbilical vein drug plasma concentrations are obtained, be recorded and the unbound drug concentration in these samples be measured.

In summary, through simulations we have shown that even when fetoplacental metabolic or placental transport clearance is small, it can significantly determine fetal drug exposure provided the magnitude of these clearance is comparable to the CL_{PD} of the drug (likely for hydrophilic drugs). In addition, we have shown that the single time point UV:MP ratio (except at steady-state after an IV infusion or when maternal concentrations do not fluctuate much after multiple oral administration), routinely reported in the literature, cannot be used as an indicator of F:M plasma drug exposure ratio even at distributional equilibrium (after single or multiple doses). Therefore, one promising alternative is to dynamically estimate fetal drug exposure in humans at term and earlier in gestation through PBPK models such as the one presented here. However, prior to using the proposed model, it needs to be verified with fetal exposure data. In our companion paper (Zhang and Unadkat, 2017), we describe such a verification using midazolam, zidovudine and theophylline.

Acknowledgements

We acknowledge Dr. Masoud Jamei for his help and support on the model. We thank Dr. Nina Isoherranen for valuable discussions.

Authorship Contributions

Participated in research design: Zhang and Unadkat

Conducted experiments: Zhang and Imperial

Contributed new reagents or analytic tool: Wedagedera, Gaohua, and Patilea-Vrana Performed data analysis: Zhang

DMD Fast Forward. Published on June 6, 2017 as DOI: 10.1124/dmd.117.075192
This article has not been copyedited and formatted. The final version may differ from this version.

References

Abduljalil K, Furness P, Johnson TN, Rostami-Hodjegan A, and Soltani H (2012) Anatomical, physiological and metabolic changes with gestational age during normal pregnancy: a database for parameters required in physiologically based pharmacokinetic modelling. *Clin Pharmacokinet* **51:**365-396.

Acharya G, Erkinaro T, Makikallio K, Lappalainen T, and Rasanen J (2004) Relationships among Doppler-derived umbilical artery absolute velocities, cardiac function, and placental volume blood flow and resistance in fetal sheep. *Am J Physiol Heart Circ Physiol* **286:**H1266-1272.

Arant BS, Jr. (1978) Developmental patterns of renal functional maturation compared in the human neonate. *J Pediatr* **92:**705-712.

Archie JG, Collins JS, and Lebel RR (2006) Quantitative standards for fetal and neonatal autopsy. *Am J Clin Pathol* **126:**256-265.

Barry M, Back D, Ormesher S, Beeching N, and Nye F (1993) Metabolism of didanosine (ddI) by erythrocytes: pharmacokinetic implications. *Br J Clin Pharmacol* **36:**87-88.

Bellotti M, Pennati G, De Gasperi C, Bozzo M, Battaglia FC, and Ferrazzi E (2004) Simultaneous measurements of umbilical venous, fetal hepatic, and ductus venosus blood flow in growth-restricted human fetuses. *Am J Obstet Gynecol* **190:**1347-1358.

Bernick SJ and Kane S (2012) Drug transfer to the fetus and to the breastfeeding infant: what do we know? *Current drug delivery* **9:**350-355.

Boito S, Struijk PC, Ursem NT, Stijnen T, and Wladimiroff JW (2002) Umbilical venous volume flow in the normally developing and growth-restricted human fetus. *Ultrasound Obstet Gynecol* **19:**344-349.

Chappuy H, Tréluyer J-M, Jullien V, Dimet J, Rey E, Fouché M, Firtion G, Pons G, and Mandelbrot L (2004a) Maternal-fetal transfer and amniotic fluid accumulation of nucleoside analogue reverse transcriptase inhibitors in human immunodeficiency virus-infected pregnant women. *Antimicrob Agents Chemother* **48:**4332-4336.

Chappuy H, Tréluyer J-M, Rey E, Dimet J, Fouché M, Firtion G, Pons G, and Mandelbrot L (2004b) Maternal-fetal transfer and amniotic fluid accumulation of protease inhibitors in pregnant women who are infected with human immunodeficiency virus. *Am J Obstet Gynecol* **191:**558-562.

Clewell RA, Merrill EA, Gearhart JM, Robinson PJ, Sterner TR, Mattie DR, and Clewell HJ, 3rd (2007) Perchlorate and radioiodide kinetics across life stages in the human: using PBPK models to predict dosimetry and thyroid inhibition and sensitive subpopulations based on developmental stage. *J Toxicol Environ Health A* **70:**408-428.

Collins JM and Unadkat JD (1989) Clinical pharmacokinetics of zidovudine. An overview of current data. *Clin Pharmacokinet* **17:**1-9.

Coonen J, Marcus M, Joosten E, van Kleef M, Neef C, van Aken H, and Gogarten W (2010) Transplacental transfer of remifentanil in the pregnant ewe. *Br J Pharmacol* **161:**1472-1476.

Coulthard MG (1985) Maturation of glomerular filtration in preterm and mature babies. *Early Hum Dev* **11:**281-292.

Cussen L, Scurry J, Mitropoulos G, McTigue C, and Gross J (1990) Mean organ weights of an Australian population of fetuses and infants. *J Paediatr Child Health* **26:**101-103.

De Sousa Mendes M, Hirt D, Vinot C, Valade E, Lui G, Pressiat C, Bouazza N, Foissac F, Blanche S, Le MP, Peytavin G, Treluyer JM, Urien S, and Benaboud S (2015) Prediction of human foetal

pharmacokinetics using ex-vivo human placenta perfusion studies and Physiologically Based models. *Br J Clin Pharmacol*.

De Sousa Mendes M, Lui G, Zheng Y, Pressiat C, Hirt D, Valade E, Bouazza N, Foissac F, Blanche S, Treluyer J-M, Urien S, and Benaboud S (2016) A Physiologically-Based Pharmacokinetic Model to Predict Human Fetal Exposure for a Drug Metabolized by Several CYP450 Pathways. *Clinical Pharmacokinetics***:**1-14.

Egan TD (1995) Remifentanil pharmacokinetics and pharmacodynamics. A preliminary appraisal. *Clin Pharmacokinet* **29:**80-94.

Else LJ, Taylor S, Back DJ, and Khoo SH (2011) Pharmacokinetics of antiretroviral drugs in anatomical sanctuary sites: the fetal compartment (placenta and amniotic fluid). *Antivir Ther* **16:**1139-1147.

FitzSimmons J, Chinn A, and Shepard TH (1988) Normal length of the human fetal gastrointestinal tract. *Pediatr Pathol* **8:**633-641.

Flo K, Wilsgaard T, and Acharya G (2010) Longitudinal reference ranges for umbilical vein blood flow at a free loop of the umbilical cord. *Ultrasound Obstet Gynecol* **36:**567-572.

Gilbert WM and Brace RA (1993) Amniotic fluid volume and normal flows to and from the amniotic cavity. *Semin Perinatol* **17:**150-157.

Gitlin D and Perricelli A (1970) Synthesis of serum albumin, prealbumin, alpha-foetoprotein, alpha-1-antitrypsin and transferrin by the human yolk sac. *Nature* **228:**995-997.

Gruenwald P and Minh HN (1961) Evaluation of body and organ weights in perinatal pathology. II. Weight of body and placenta of surviving and of autopsied infants. *Am J Obstet Gynecol* **82:**312-319.

Guignard JP, Torrado A, Da Cunha O, and Gautier E (1975) Glomerular filtration rate in the first three weeks of life. *J Pediatr* **87:**268-272.

Hansen K, Sung CJ, Huang C, Pinar H, Singer DB, and Oyer CE (2003) Reference values for second trimester fetal and neonatal organ weights and measurements. *Pediatr Dev Pathol* **6:**160-167.

Hansen NB, Oh W, LaRochelle F, and Stonestreet BS (1983) Effects of maternal ritodrine administration on neonatal renal function. *J Pediatr* **103:**774-780.

Haugen G, Kiserud T, Godfrey K, Crozier S, and Hanson M (2004) Portal and umbilical venous blood supply to the liver in the human fetus near term. *Ultrasound Obstet Gynecol* **24:**599-605.

Hill MD and Abramson FP (1988) The significance of plasma protein binding on the fetal/maternal distribution of drugs at steady-state. *Clin Pharmacokinet* **14:**156-170.

Isoherranen N and Thummel KE (2013) Drug metabolism and transport during pregnancy: how does drug disposition change during pregnancy and what are the mechanisms that cause such changes? *Drug Metab Dispos* **41:**256-262.

Kanto J, Sjovall S, Erkkola R, Himberg JJ, and Kangas L (1983) Placental transfer and maternal midazolam kinetics. *Clin Pharmacol Ther* **33:**786-791.

Ke AB, Nallani SC, Zhao P, Rostami-Hodjegan A, Isoherranen N, and Unadkat JD (2013a) A physiologically based pharmacokinetic model to predict disposition of CYP2D6 and CYP1A2 metabolized drugs in pregnant women. *Drug Metab Dispos* **41:**801-813.

Ke AB, Nallani SC, Zhao P, Rostami-Hodjegan A, and Unadkat JD (2012) A PBPK Model to Predict Disposition of CYP3A-Metabolized Drugs in Pregnant Women: Verification and Discerning the Site of CYP3A Induction. *CPT Pharmacometrics Syst Pharmacol* **1:**e3.

Ke AB, Nallani SC, Zhao P, Rostami-Hodjegan A, and Unadkat JD (2013b) Expansion of a PBPK Model to Predict Disposition in Pregnant Women of Drugs Cleared via Multiple CYP Enzymes, Including CYP2B6, CYP2C9 and CYP2C19. *Br J Clin Pharmacol*.

Ke AB, Nallani SC, Zhao P, Rostami-Hodjegan A, and Unadkat JD (2014) Expansion of a PBPK model to predict disposition in pregnant women of drugs cleared via multiple CYP enzymes, including CYP2B6, CYP2C9 and CYP2C19. *Br J Clin Pharmacol* **77:**554-570.

Kenny JF, Plappert T, Doubilet P, Saltzman DH, Cartier M, Zollars L, Leatherman GF, and St John Sutton MG (1986) Changes in intracardiac blood flow velocities and right and left ventricular stroke volumes with gestational age in the normal human fetus: a prospective Doppler echocardiographic study. *Circulation* **74:**1208-1216.

Kessler J, Rasmussen S, Godfrey K, Hanson M, and Kiserud T (2008) Longitudinal study of umbilical and portal venous blood flow to the fetal liver: low pregnancy weight gain is associated with preferential supply to the fetal left liver lobe. *Pediatr Res* **63:**315-320.

Kiserud T, Rasmussen S, and Skulstad S (2000) Blood flow and the degree of shunting through the ductus venosus in the human fetus. *Am J Obstet Gynecol* **182:**147-153.

Knupp CA, Shyu WC, Dolin R, Valentine FT, McLaren C, Martin RR, Pittman KA, and Barbhaiya RH (1991) Pharmacokinetics of didanosine in patients with acquired immunodeficiency syndrome or acquired immunodeficiency syndrome-related complex. *Clin Pharmacol Ther* **49:**523-535.

Krauer B, Dayer P, and Anner R (1984) Changes in serum albumin and alpha 1-acid glycoprotein concentrations during pregnancy: an analysis of fetal-maternal pairs. *Br J Obstet Gynaecol* **91:**875-881.

Lees C, Albaiges G, Deane C, Parra M, and Nicolaides KH (1999) Assessment of umbilical arterial and venous flow using color Doppler. *Ultrasound Obstet Gynecol* **14:**250-255.

Loccisano AE, Longnecker MP, Campbell JL, Jr., Andersen ME, and Clewell HJ, 3rd (2013) Development of PBPK models for PFOA and PFOS for human pregnancy and lactation life stages. *J Toxicol Environ Health A* **76:**25-57.

Marzolini C and Kim RB (2005) Placental transfer of antiretroviral drugs. *Clin Pharmacol Ther* **78:**118-122.

Mathias AA, Hitti J, and Unadkat JD (2005) P-glycoprotein and breast cancer resistance protein expression in human placentae of various gestational ages. *Am J Physiol Regul Integr Comp Physiol* **289:**R963-969.

Mayhew TM, Ohadike C, Baker PN, Crocker IP, Mitchell C, and Ong SS (2003) Stereological investigation of placental morphology in pregnancies complicated by pre-eclampsia with and without intrauterine growth restriction. *Placenta* **24:**219-226.

McCormack SA and Best BM (2014) Protecting the Fetus Against HIV Infection: A Systematic Review of Placental Transfer of Antiretrovirals. *Clin Pharmacokinet* **53:**989-1004.

McGowan JP and Shah SS (2000) Prevention of perinatal HIV transmission during pregnancy. *J Antimicrob Chemother* **46:**657-668.

Mitchell AA, Gilboa SM, Werler MM, Kelley KE, Louik C, and Hernandez-Diaz S (2011) Medication use during pregnancy, with particular focus on prescription drugs: 1976-2008. *Am J Obstet Gynecol* **205:**51 e51-58.

Moniz CF, Nicolaides KH, Bamforth FJ, and Rodeck CH (1985) Normal reference ranges for biochemical substances relating to renal, hepatic, and bone function in fetal and maternal plasma throughout pregnancy. *J Clin Pathol* **38:**468-472.

monograph D.

Myllynen P, Immonen E, Kummu M, and Vahakangas K (2009) Developmental expression of drug metabolizing enzymes and transporter proteins in human placenta and fetal tissues. *Expert Opin Drug Metab Toxicol* **5:**1483-1499.

Myllynen P, Pasanen M, and Vahakangas K (2007) The fate and effects of xenobiotics in human placenta. *Expert Opin Drug Metab Toxicol* **3:**331-346.

Nagata S, Koyanagi T, Horimoto N, Satoh S, and Nakano H (1990) Chronological development of the fetal stomach assessed using real-time ultrasound. *Early Hum Dev* **22:**15-22.

Ngan Kee WD, Khaw KS, Tan PE, Ng FF, and Karmakar MK (2009) Placental transfer and fetal metabolic effects of phenylephrine and ephedrine during spinal anesthesia for cesarean delivery. *Anesthesiology* **111:**506-512.

Parulekar SG (1991) Sonography of normal fetal bowel. *J Ultrasound Med* **10:**211-220.

Pereira CM, Nosbisch C, Winter HR, Baughman WL, and Unadkat JD (1994) Transplacental pharmacokinetics of dideoxyinosine in pigtailed macaques. *Antimicrob Agents Chemother* **38:**781-786.

Pidoux G, Gerbaud P, Guibourdenche J, Therond P, Ferreira F, Simasotchi C, Evain-Brion D, and Gil S (2015) Formaldehyde Crosses the Human Placenta and Affects Human Trophoblast Differentiation and Hormonal Functions. *PLoS One* **10:**e0133506.

Poet TS, Kirman CR, Bader M, van Thriel C, Gargas ML, and Hinderliter PM (2010) Quantitative risk analysis for N-methyl pyrrolidone using physiologically based pharmacokinetic and benchmark dose modeling. *Toxicol Sci* **113:**468-482.

Polin RA, Fox WW, and Abman SH (2004) *Fetal and neonatal physiology*. W.B. Saunders Co., Philadelphia, Pa.

Ron M, Hochner-Celnikier D, Menczel J, Palti Z, and Kidroni G (1984) Maternal-fetal transfer of aminophylline. *Acta Obstet Gynecol Scand* **63:**217-218.

Rubesova E, Vance CJ, Ringertz HG, and Barth RA (2009) Three-dimensional MRI volumetric measurements of the normal fetal colon. *AJR Am J Roentgenol* **192:**761-765.

Rudolph AM, Heymann MA, Teramo KAW, Barrett CT, and Raiha NCR (1971) Studies on the Circulation of the Previable Human Fetus. *Pediatr Res* **5:**452-465.

Sutton MS, Theard MA, Bhatia SJ, Plappert T, Saltzman DH, and Doubilet P (1990) Changes in placental blood flow in the normal human fetus with gestational age. *Pediatr Res* **28:**383-387.

Tchirikov M, Rybakowski C, Huneke B, Schoder V, and Schroder HJ (2002) Umbilical vein blood volume flow rate and umbilical artery pulsatility as 'venous-arterial index' in the prediction of neonatal compromise. *Ultrasound Obstet Gynecol* **20:**580-585.

Tchirikov M, Rybakowski C, Huneke B, and Schroder HJ (1998) Blood flow through the ductus venosus in singleton and multifetal pregnancies and in fetuses with intrauterine growth retardation. *Am J Obstet Gynecol* **178:**943-949.

Tuntland T, Nosbisch C, Baughman WL, Massarella J, and Unadkat JD (1996) Mechanism and rate of placental transfer of zalcitabine (2',3'-dideoxycytidine) in Macaca nemestrina. *Am J Obstet Gynecol* **174:**856-863.

Tuntland T, Odinecs A, Pereira CM, Nosbisch C, and Unadkat JD (1999) In vitro models to predict the in vivo mechanism, rate, and extent of placental transfer of dideoxynucleoside drugs against human immunodeficiency virus. *Am J Obstet Gynecol* **180:**198-206.

Unadkat JD, Dahlin A, and Vijay S (2004) Placental drug transporters. *Curr Drug Metab* **5:**125-131.

van den Anker JN, de Groot R, Broerse HM, Sauer PJ, van der Heijden BJ, Hop WC, and Lindemans J (1995) Assessment of glomerular filtration rate in preterm infants by serum creatinine: comparison with inulin clearance. *Pediatrics* **96:**1156-1158.

van der Sandt IC, Vos CM, Nabulsi L, Blom-Roosemalen MC, Voorwinden HH, de Boer AG, and Breimer DD (2001) Assessment of active transport of HIV protease inhibitors in various cell lines and the in vitro blood--brain barrier. *AIDS* **15:**483-491.

Veille JC, Hanson RA, Tatum K, and Kelley K (1993) Quantitative assessment of human fetal renal blood flow. *Am J Obstet Gynecol* **169:**1399-1402.

Velasque LS, Estrela RCE, Suarez-Kurtz G, and Struchiner CJ (2007) A new model for the population pharmacokinetics of didanosine in healthy subjects. *Braz J Med Biol Res* **40:**97-104.

Wang Y, Zhao,S. (2010) Vascular Biology of the Placenta San Rafael (CA): Morgan & Claypool Life Sciences.

Weiner CP, Sipes SL, and Wenstrom K (1992) The effect of fetal age upon normal fetal laboratory values and venous pressure. *Obstet Gynecol* **79:**713-718.

Yoon M, Schroeter JD, Nong A, Taylor MD, Dorman DC, Andersen ME, and Clewell HJ, 3rd (2011) Physiologically based pharmacokinetic modeling of fetal and neonatal manganese exposure in humans: describing manganese homeostasis during development. *Toxicol Sci* **122:**297-316.

Zhang Z and Unadkat JD (2017) Verification of a Maternal-Fetal Physiologically Based Pharmacokinetic Model for Passive Placental Permeability Drugs. *Drug Metabolism and Disposition*.

Footnotes

The current work was supported by National Institute of Health National Institute on Drug Abuse [Grant P01DA032507]. ZZ was supported by the Office of Women's Health, US Food and Drug Administration [ORISE fellowship] for part of the submitted work. There are no other relationships or activities that could appear to have influenced the submitted work

DMD Fast Forward. Published on June 6, 2017 as DOI: 10.1124/dmd.117.075192
This article has not been copyedited and formatted. The final version may differ from this version.

Figure Legends

Figure 1: Schematic diagram of the maternal-fetal full PBPK model. Solid arrows indicate tissue blood flows, whereas dashed arrows indicate clearances. CL: clearance; Prefixes: f-fetal; Subscripts: PD- passive diffusion, M- maternal, P- placental, F- fetal, A- amniotic fluid, met-metabolism, renal-renal excretion, reabsorp- amniotic fluid swallowing. $CL_{PF/FP}$ and $CL_{PM/MP}$ represent unidirectional transporter-mediated clearances.

Figure 2: **Impact of changes in maternal clearance (CL_{m0}) on fetal and maternal drug X plasma concentration and UV:MP ratio.** Changes in maternal systemic clearance (CL_{m0}) of drug X significantly influenced maternal-fetal drug X plasma concentration-time profiles at week 40. Following IV infusion (16.7 mg/h) at week 40, decreasing CL_{m0} from 45 L/h (red) to 4.5 L/h (blue) increased the steady-state maternal (solid lines) and fetal (dashed lines) plasma concentration of drug X as well as the time to reach steady-state (**a**). Inset shows the curves on a semi-logarithmic scale. The corresponding UV:MP ratios indicate that, at steady-state$_{inf}$, these ratios do not change with changes in CL_{m0} (45L/h, red; 4.5L/h, blue) (**b**). Following a single oral dose (400 mg), increasing CL_{m0} from 4.5L/h (blue) to 45 L/h (red) resulted in lower maternal plasma drug concentrations (solid lines) and subsequently lower fetal plasma drug X concentrations (dashed lines) (**c**). Corresponding changes in UV:MP ratio indicate that higher CL_{m0} (red) led to greater time-dependent fluctuations in the UV:MP ratio as well as a lager UV:MP ratio at distributional equilibrium (**d**). Under a multiple oral dosing regimen (133.3mg; τ =8 h) lower CL_{m0} (blue) not only prolonged the time to reach steady-state but also resulted in greater extent of drug accumulation (**e**). In addition, lower CL_{m0} (blue) led to less fluctuations in UV:MP ratio within a dosing interval compared with higher CL_{m0} (red) (**f**). When the dosing

DMD Fast Forward. Published on June 6, 2017 as DOI: 10.1124/dmd.117.075192
This article has not been copyedited and formatted. The final version may differ from this version.

interval was increased (400 mg; τ =24 h), the effect of reduction in CL_{m0} on drug accumulation (**g**) or variation in UV:MP ratio (**h**) was dampened. In panels **e** and **g**, predicted F;M AUC ratio remained unity despite the changes in CL_{m0}. See **Table 3** for the clearance values used in these simulations.

Figure 3: Impact of changes in maternal clearance (CL_{m0}) on fetal and maternal drug Y plasma concentration and UV:MP ratio. Changes in maternal systemic clearance (CL_{m0}) of drug Y significantly influenced maternal-fetal drug Y plasma concentration-time profiles at week 40. Following IV infusion (0.625 mg/h) at week 40, a 10-fold decrease in maternal hepatic intrinsic clearance (from 3327L/h to 332.7L/h) resulted in a decrease in CL_{m0} from 43 L/h (red) to 12 L/h (blue). The resultant steady-state$_{inf}$ maternal (solid lines) and fetal (dashed lines) plasma concentration of drug Y as well as the time to reach steady-state increased (**a**). The corresponding UV:MP ratios indicate that, at steady-state$_{inf}$, these ratios stay at 1.2 and do not change with varying CL_{m0} (43L/h, red; 12L/h, blue) (**b**). Following a single oral dose (15 mg), increasing CL_{m0} from 12 L/h (blue) to 43 L/h (red) resulted in lower maternal plasma drug concentrations (solid lines) and subsequently lower fetal plasma drug X concentrations (dashed lines)(**c**). Corresponding changes in UV:MP ratio indicate that higher CL_{m0} (red) led to greater fluctuations in the UV:MP ratio as well as a larger UV:MP ratio at distributional equilibrium (**d**). After multiple oral dosing (3.75 mg; τ =4 h) lower CL_{m0} (blue) not only prolonged the time to reach steady-state but also resulted in much greater drug accumulation (**e**). In addition, lower CL_{m0} (blue) led to less fluctuations in UV:MP ratio (within a dosing interval) when compared with higher CL_{m0} (red) (**f**). When the dosing interval was increased (15 mg; τ =24 h), the effect of reduction in CL_{m0} on dose accumulation (**g**) or variations in UV:MP ratio(**h**) was dampened.

DMD Fast Forward. Published on June 6, 2017 as DOI: 10.1124/dmd.117.075192
This article has not been copyedited and formatted. The final version may differ from this version.

Inset shows the curves on a semi-logarithmic scale. In panels **e** and **g**, predicted unbound F:M AUC ratio remained unity despite the changes in CL_{m0}. See **Table 4** for the clearance values used in these simulations.

Figure 4: Impact of changes in transplacental passive diffusion clearance (CL_{PD}) on fetal and maternal drug X plasma concentration and UV:MP ratio. Changes in transplacental passive diffusion clearance (CL_{PD}) of drug X significantly influenced fetal (dashed lines), but not maternal (solid lines), drug X plasma concentration-time profile at week 40. Following IV infusion (16.7 mg/h) at week 40, decreasing CL_{PD} from 18 L/h (red) to 1.8 L/h (blue) did not affect the maternal (the red and blue solid lines overlap) or fetal steady-state$_{inf}$ plasma concentrations of the drug (**a**). The corresponding UV:MP ratios indicate that, at steady-state$_{inf}$, these ratios do not change with alterations in CL_{PD} (18L/h, red; 1.8L/h, blue) but the time to reach the steady-state ratio was prolonged (**a**,**b**). Following a single oral dose (400 mg), increasing CL_{PD} from 1.8L/h (blue) to 18L/h (red) significantly modified the shape of fetal plasma C-T curves (dashed lines) but not maternal plasma drug concentrations (solid lines; blue and red lines overlap) (**c**). Corresponding changes in UV:MP ratio indicate that higher CL_{PD} (red) not only shortened the time to reach distributional equilibrium but also reduced distributional equilibrium UV:MP ratio compared with lower CL_{PD} (blue) (**d**). After multiple oral doses (400 mg; τ =24h), alterations in CL_{PD} did not affect maternal plasma drug X C-T curve but significantly changed the shape of fetal plasmas drug X C-T profile. Higher CL_{PD} (red) resulted greater fluctuations in fetal plasma drug X concentration within a dosing interval compared with lower CL_{PD} (blue) (**e**). In contrast, higher CL_{PD} (red) produced less fluctuations in UV:MP ratio within a dosing interval compared with lower CL_{PD} (blue) (**f**). Insets in (**d**) and (**f**) show the F:M

DMD Fast Forward. Published on June 6, 2017 as DOI: 10.1124/dmd.117.075192
This article has not been copyedited and formatted. The final version may differ from this version.

AUC ratios at lower CL_{PD} (blue) or higher CL_{PD} (red). The predicted F;M AUC ratio remained unity despite changes in CL_{PD} following single (**c**) or multiple oral doses (**e**) of drug X. See **Table 3** for the clearance values used in these simulations.

Figure 5: Impact of changes in transplacental passive diffusion clearance (CL_{PD}) on fetal and maternal drug Y plasma concentration and UV:MP ratio. Changes in transplacental passive diffusion clearance (CL_{PD}) of drug Y significantly influenced drug Y fetal (dashed lines), but not maternal (solid lines), plasma concentration-time profile at week 40. Following IV infusion (0.625 mg/h) at week 40, decreasing CL_{PD} from 22.5 L/h (red) to 2.25 L/h (blue) did not affect the maternal (the red and blue solid lines overlap) or fetal steady-state$_{inf}$ plasma concentration of the drug (**a**). The corresponding UV:MP ratios indicate that, at steady-state$_{inf}$, these ratios do not change with alterations in CL_{PD} (22.5L/h, red; 2.25L/h, blue) but the time to reach the steady-state ratio was prolonged (**b**). Following a single oral dose (15 mg), decreasing CL_{PD} from 22.5 L/h (red) to 2.25 L/h (blue) significantly modified the shape of fetal plasma C-T curve (dashed lines) but not maternal plasma drug concentrations (solid lines; blue and red lines overlap) (**c**). Corresponding changes in UV:MP ratio indicate that higher CL_{PD} (red) not only shortened the time to reach distributional equilibrium but also reduced distributional equilibrium UV:MP ratio compared with lower CL_{PD} (blue) (**d**). Under a multiple oral dosing regimen (15 mg; τ =24h), alterations in CL_{PD} did not affect maternal plasma drug Y C-T curve but significantly changed the shape of fetal plasmas drug Y C-T profile. Higher CL_{PD} (red) resulted greater fluctuations in fetal plasma drug Y concentration within a dosing interval compared with lower CL_{PD} (blue) (**e**). In contrast, higher CL_{PD} (red) produced less fluctuations in UV:MP ratio within a dosing interval compared with lower CL_{PD} (blue) as transplacental distributional

DMD Fast Forward. Published on June 6, 2017 as DOI: 10.1124/dmd.117.075192
This article has not been copyedited and formatted. The final version may differ from this version.

equilibirum of drug Y was quickly attained following an oral dose (**f**). Insets in (**d**) and (**f**) show the unbound F:M AUC ratios at lower CL_{PD} (blue) or higher CL_{PD} (red). The predicted unbound F:M AUC ratio remained unity despite changes in CL_{PD} following single (**c**) or multiple oral doses (**e**) of drug Y. See **Table 4** for the clearance values used in these simulations.

Figure 6: Impact of changes in feto-placental metabolism and placental transport on fetal plasma and placental drug X concentration, P:M AUC, F:M AUC and UV:MP ratio following a single 400mg oral dose of drug X. Changes in fetoplacental clearance pathways differentially impacted fetal exposure to drug X, placental:maternal plasma (P:M) AUC ratio (hatched bar), fetal:maternal (F:M) plasma AUC ratio (solid bar), and the UV:MP ratio after a single 400 mg oral dose of drug X at week 40. The placental passive diffusion clearance (CL_{PD}) of drug X was held at 1.8L/h. The clearance pathway varied is indicated at the extreme left of the first panel of each row. The indicated clearance was set at 0 L/h, 0.18 L/h, 0.9 L/h, or 1.8 L/h, respectively (0%, 10%, 50%, or 100% of CL_{PD}; black, red, green, and blue lines, respectively). Other than CL_{MP} (**d1**), increasing any of the indicated clearance pathways resulted in lower fetal plasma drug X concentrations (**a1-c1** and **e1**). When CL_{f0} was present, the resultant F:M plasma AUC ratio was lower (**b2** and **c2**) than when only CL_{P0} was present (**a2**). In all cases the predicted UV:MP ratio at distributional equilibrium was significantly greater than its $steady\text{-}state_{inf}$ value (**Supplementary Information Eq. 1**). The UV:MP ratio at distributional equilibrium decreased with increase in CL_{p0}, $CL_{f0,}CL_{f0}$ plus CL_{p0}, or CL_{PM} (**a3**, **b3**,**c3**,and **e3**,respectively) and increased with an increase in CL_{MP} (**d3**). See **Table 3** for the clearance values used in these simulations.

DMD Fast Forward. Published on June 6, 2017 as DOI: 10.1124/dmd.117.075192
This article has not been copyedited and formatted. The final version may differ from this version.

Figure 7: **Impact of changes in feto-placental metabolism and placental transport on fetal plasma and placental drug Y concentration, P:M AUC, F:M AUC and UV:MP ratio following a single 15 mg oral dose of drug Y.** Changes in fetoplacental clearance pathways differentially impacted fetal exposure to drug Y, placental:maternal plasma (P:M) unbound AUC ratio (hatched bar), fetal:maternal (F:M) plasma unbound AUC ratio (solid bar), and the UV:MP ratio after a single 15 mg oral dose of drug Y at week 40. The placental passive diffusion clearance (CL_{PD}) of drug Y was held at 22.5 L/h. The clearance pathway varied is indicated at the extreme left of the first panel of each row. The indicated clearance was set at 0 L/h, 2.25 L/h, 11.3 L/h, or 22.5 L/h, respectively (0%, 10%, 50%, or 100% of CL_{PD}; black, red, green, and blue lines, respectively). Other than CL_{MP} (**d1**), increasing any of the indicated clearance pathways resulted in lower fetal plasma drug X concentrations (**a1-c1** and **e1**). When CL_{f0} was present, the F:M plasma unbound AUC ratio was lower (**b2** and **c2**) than when only CL_{P0} was present (**a2**). In all cases the predicted UV:MP ratio at distributional equilibrium was greater than its expected steady-state$_{inf}$ value (**Supplementary Information Eq. 1**). The UV:MP ratio at distributional equilibrium decreased with increase in CL_{p0}, $CL_{f0,}CL_{f0}$ plus CL_{p0}, or CL_{PM} (**a3**, **b3**,**c3**,and **e3**,respectively) and increased with an increase in CL_{MP} (**d3**). See **Table 4** for the clearance values used in these simulations.

Figure 8: Impact of gestational age on maternal and fetal drug X plasma conc. and F:M AUC ratio following a single 400 mg oral dose of drug X at week 20 (red) or week 40 (blue). The effect of gestational age on fetal exposure to drug X varies with fetoplacental clearance mechanisms involved. Maternal (solid) and fetal (dashed) C-T profiles as well as fetal:maternal (F:M) plasma AUC ratios were simulated after a single 400mg oral dose of drug X at week 20

(red) and week 40 (blue) under different scenarios. In scenario 1, where no irreversible loss of drug X occurred in the fetoplacental unit, the advancement of gestational age did not significantly affect fetal-maternal drug disposition (**a**) or the F:M plasma AUC ratio of unity (**b**). In scenario 2, the addition of fetal metabolism (increased proportionally with the fetal body volume as gestational age increased) significantly reduced fetal plasma drug concentrations (**c** vs. **a**) and resulted in ~50% decrease in F:M AUC plasma ratio at both gestational ages (**d**). In scenario 3, placental P-gp efflux clearance decreased with gestational age (based on reported P-gp expression and changes in placental volume with gestational age). Consequently, fetal exposure to drug X increased with gestational age, reflected by higher fetal plasma drug concentrations (**e**) and increased F:M plasma AUC ratio (**f**). Finally, in scenario 4 where both fetal metabolism and placental efflux were present, further reduction in fetal exposure was observed at both gestational ages (**g, h**). See **Table 3** and **Table 5** for the clearance values used in these simulations.

Figure 9: Impact of gestational age on maternal and fetal drug Y plasma concentration and F:M AUC ratio following a single 15 mg oral dose of drug Y at week 20 (red) and week 40 (blue). The effect of gestational age on fetal exposure to drug Y varies with fetoplacental clearance mechanisms involved. Maternal (solid) and fetal (dashed) C-T profiles, maternal (solid) and fetal (hatched) plasma AUCs, as well as fetal:maternal (F:M) [total (solid) and unbound (hatched)] AUC ratios were simulated after a single 15 mg oral dose of drug Y at week 20 (red) and week 40 (blue) under different scenarios. In scenario 1, where no irreversible loss of drug Y occurred in the fetoplacental unit under a constant maternal hepatic unbound intrinsic clearance ($CL_{int,u,hep}$), advancement of gestational age resulted in increased fetal plasma AUC

DMD Fast Forward. Published on June 6, 2017 as DOI: 10.1124/dmd.117.075192
This article has not been copyedited and formatted. The final version may differ from this version.

despite the decrease in maternal plasma AUC (**a**, **b**) but did not affect the F:M plasma AUC unbound ratio of unity (**c**). In scenario 2, the assumed 100% higher $CL_{int,u,hep}$ at week 40 compared with week 20 significantly decreased maternal-fetal plasma drug Y concentrations (hence AUCs) at term (**d** vs **a**; **e** vs **b**) while F:M AUC plasma ratios at both gestational ages were identical to those in scenario 1 (**f** vs **c**). In scenario 3, placental P-gp-mediated efflux clearance decreased with gestational age. Consequently, fetal exposure to drug Y increased with gestational age, reflected by higher fetal plasma drug concentrations (**g**) and increased F:M plasma AUC ratio (**i**). Finally, in scenario 4, increase in fetal exposure from week 20 to week 40 persisted in the presence of both decrease in placental efflux and increase in CL_{m0} with gestational age, but to a smaller extent compared to scenario 3 (**k** vs **h**). Note that F:M AUC plasma ratios at both gestational ages were identical to those in scenario 3 (**l** vs **i**). See **Table 4** and **Table 5** for the clearance values used in these simulations.

Table 1: Gestational age-dependent kay fetal and selected maternal physiological parameters

Parameter (units)	Formula [a]	Reference(s)	Graph
Maternal placental blood flow (L/h)[c]	$1.71 + 0.207GA + 0.0841GA^2 - 0.0015GA^3$ ($R^2 = 0.991$, RSE = 2.54, N = 5; GA: 0-40 weeks)	(Abduljalil et al., 2012)	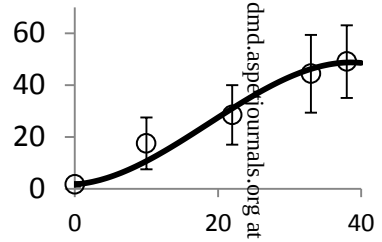
Fetal serum albumin (g/L)	$-31.7 + 4.35GA - 0.101GA^2 + 0.0009GA^3$ ($R^2 = 0.987$, RSE = 1.44, N = 15; GA: 10-40 weeks)	(Gitlin and Perricelli, 1970; Krauer et al., 1984; Moniz et al., 1985; Weiner et al., 1992)	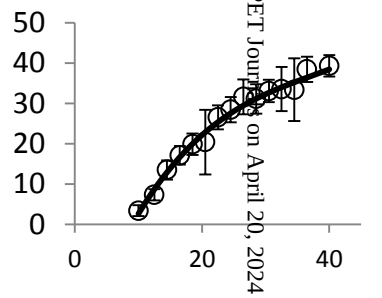
Fetal serum α_1-acid glycoprotein (g/L)	$0.02e^{0.0616GA}$ ($R^2 = 0.519$, RSE = 0.0669, N = 19; GA: 16-38 weeks)	(Krauer et al., 1984)	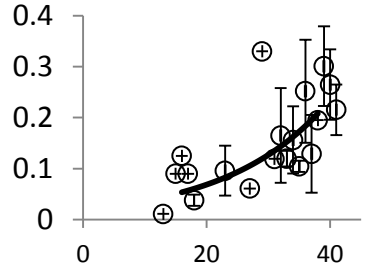

Fetal brain volume (mL)	$36.0 - 7.53GA + 0.400GA^2$ ($R^2 = 0.998$, RSE = 5.83, N = 15; GA: 12-41 weeks)	(Archie et al., 2006; Cussen et al., 1990; Gruenwald and Minh, 1961; Hansen et al., 2003)	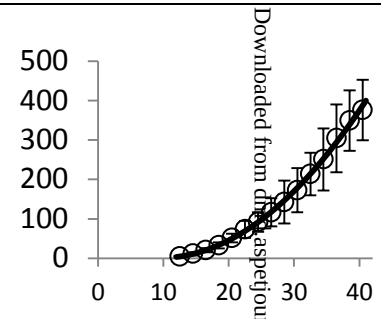
Fetal liver volume (mL)	$16.6 - 2.92GA + 0.143GA^2$ ($R^2 = 0.996$, RSE = 2.93, N = 15; GA: 12-41 weeks)	(Archie et al., 2006; Cussen et al., 1990; Gruenwald and Minh, 1961; Hansen et al., 2003)	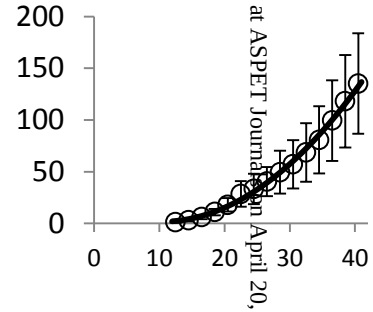
Fetal stomach volume (mL)	$0.127e^{0.101GA}$ ($R^2 = 0.962$, RSE = 0.184, N = 18; GA: 20-37 weeks) $25.3 - 0.548GA$ ($R^2 = 0.994$, RSE = 0.0572, N = 3; GA: >37 weeks)	(Nagata et al., 1990)	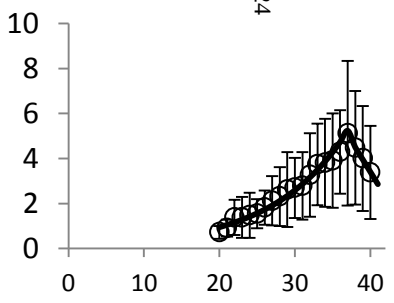

Fetal small intestine volume (mL)[d]	$0.0203e^{0.194GA}$ (R^2 = 0.998, RSE = 0.0688, N = 36; GA: 12-25 weeks)	(Archie et al., 2006; FitzSimmons et al., 1988; Nagata et al., 1990; Parulekar, 1991)	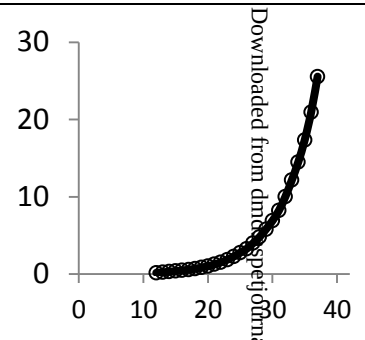
Fetal large intestine volume (mL)	$0.078e^{0.169GA}$ (R^2 = 0.866, RSE = 7.44, N = 44; GA: 20-37 weeks)	(Rubesova et al., 2009)	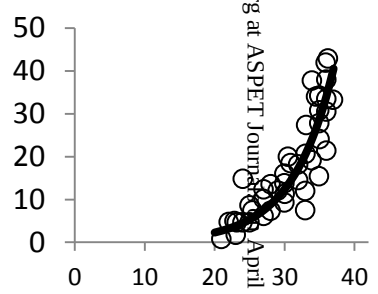
Fetal total gut volume (mL) [e]	$-54.3 + 8.90GA - 0.479GA^2 + 0.0088GA^3$ (R^2 = 0.998, RSE ≈ 0, N = 28; GA: 13-37 weeks)	(Archie et al., 2006; Nagata et al., 1990; Parulekar, 1991; Rubesova et al., 2009)	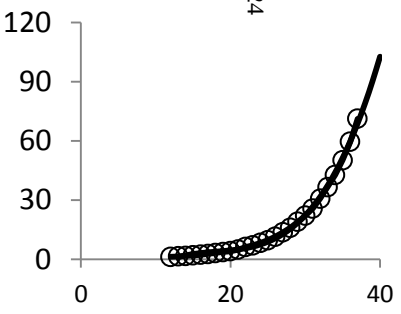

Fetal kidney volume (mL)	2.37 - 0.619GA + 0.0335GA^2 (R^2 = 0.994, RSE = 0.994, N = 15; GA: 14-41 weeks)	(Cussen et al., 1990; Hansen et al., 2003)	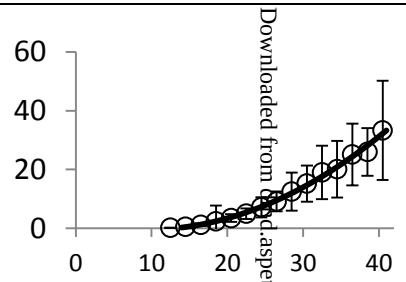
Fetal umbilical blood flow (L/h)	0.647 - 0.227GA + 0.0179GA^2 (R^2 = 0.9984, RSE = 0.235, N = 23; GA: 18-40 weeks)	(Acharya et al., 2004; Boito et al., 2002; Flo et al., 2010; Kiserud et al., 2000; Lees et al., 1999; Sutton et al., 1990;	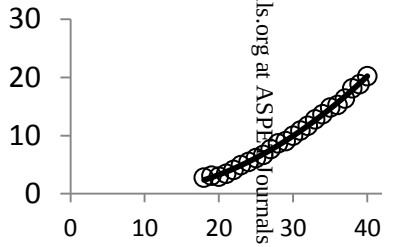
Ductus venosus blood flow (L/h) [f]	2.05 - 0.297GA + 0.0116GA^2 (R^2 = 1.00; GA: 20-38 weeks) [g]	(Bellotti et al., 2004; Kessler et al., 2008)	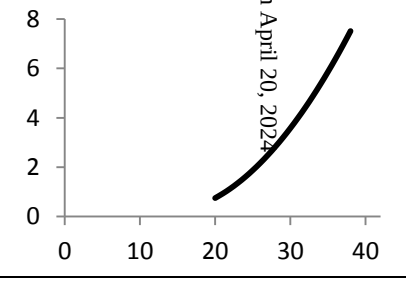
Fetal portal vein blood flow (L/h)	0.714 + 0.0489GA + 0.0008GA^2 (R^2= 1.00; GA: 20-38 weeks) [g]	(Bellotti et al., 2004; Haugen et al., 2004; Kessler et al., 2008)	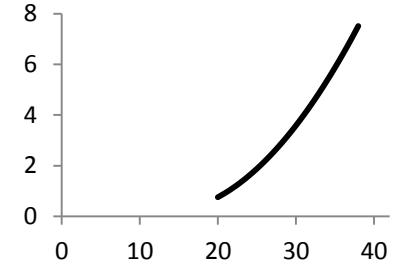

Fetal brain blood flow (mL/min)	$5.56e^{0.0921GA}$ (R^2 = 0.04, RSE = 10.8, N = 32; GA: 10-20 weeks) [h]	(Kenny et al., 1986; Rudolph et al., 1971)	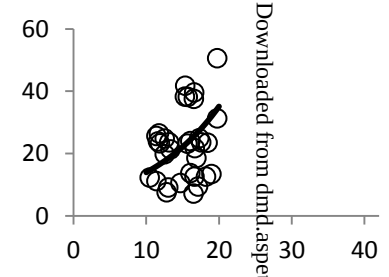
Fetal kidney blood flow (mL/min)	$2.18e^{0.0865GA}$ (R^2 = 0.707, RSE = 18.3, N = 66; GA: 10-41 weeks) [h]	(Kenny et al., 1986; Rudolph et al., 1971; Veille et al., 1993)	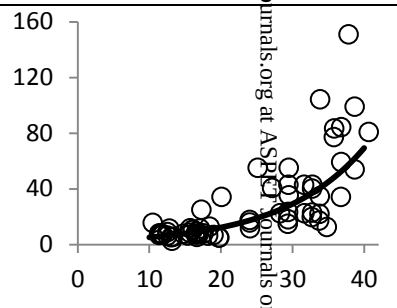
Fetal glomerular filtration clearance (L/h) [i]	$0.00046e^{0.15GA}$ (R^2 = 0.69, RSE = 0.03, N = 16; GA: 23-40 weeks)	(Arant, 1978; Coulthard, 1985; Hansen et al., 1983; van den Anker et al., 1995)	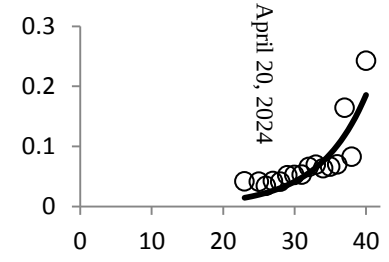
Fetal gut blood flow (mL/min)	$1.67e^{0.124GA}$ (R^2= 0.999, RSE = 4.67, N = 32; GA: 10-20 weeks) [h]	(Kenny et al., 1986; Rudolph et al., 1971; Veille et al., 1993)	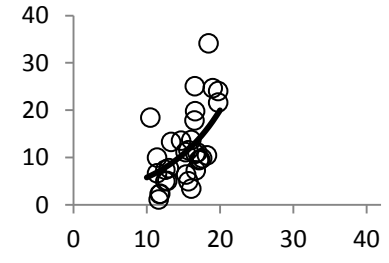

Fetal rest of body compartment volume (mL)[j]	290.0 - 62.5GA+ 3.22GA^2 (R^2 = 0.998)	(Abduljalil et al., 2012)	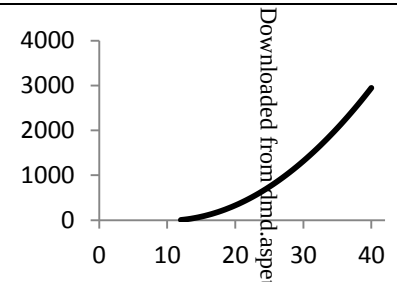
Syncytiotrophoblast volume (mL)	- 6.83 + 0.650GA + 0.0370GA^2 (R^2 = 0.757, RSE = 3.86, N = 6; GA: 10-41 weeks)	(Mayhew et al., 2003)	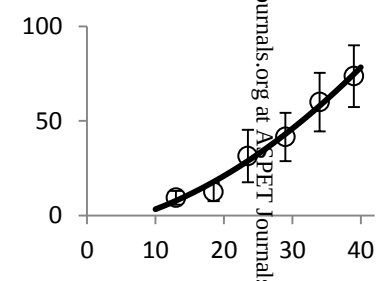
Placental villous surface area (m^2)	4.66 - 0.788GA + 0.0383GA^2 - 0.0004GA^3 (R^2 = 0.922, RSE = 1.008, N = 23; GA: 12-41 weeks)	(Wang, 2010)	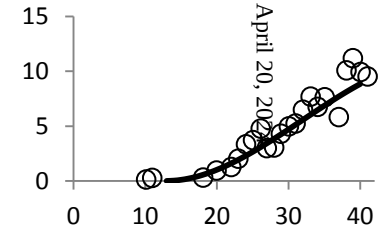

a. GA denotes gestational age in weeks.

b. In the graphs above, the x axes are gestational age (GA) in weeks, whereas the y axes show the gestational age-dependent trends of the respective parameters in units as indicated in the first cell of each row. The GA-specific average values (overall mean across studies ± overall S.D) are overlaid when applicable. Residual standard error (RSE) and N (the number of overall means across gestational ages) are also provided in the formula column when relevant.

c. Average maternal placental blood flow values at various GA and the resultant equation were those from the meta-analysis performed by Abduljalil et al..

d. Calculated using a reported fetal small intestine (SI) diameter formula (Parulekar 1991) and the reported fetal SI length (FitzSimmons, Chinn et al. 1988) assuming cylindrical SI and negligible gut wall thickness.

e. Fetal gut consists of fetal stomach, small intestine, and large intestine. Unfortunately, there is no reported data on fetal small intestine volume during the second half of gestation. Because the reported data on these three organs overlapped between week 20 and week 25, the small intestine volume percentage (SI %) of the total gut volume for only this range of gestation was fitted to various models. A linear model (SI% = 0.652GA+11.766), best describing the gestational age dependency of SI% volume within this range, was used to estimate the SI% volume beyond week 25. Then, the total fetal gut volume after week 25 was calculated by dividing the sum of fetal stomach and large intestine volumes by their corresponding volume percentage (i.e. 1 - SI%).

f. Calculated as the difference between total liver venous blood flow and umbilical venous blood flow.

g. The average values computed from published GA-dependent formulae were used as individual measurements were not available.

h. Calculated as the product of fetal combined cardiac output (CCO) (Rudolph et al., 1971) and the percent CCO [before week 20 (Kenny et al., 1986) and after week 20 (Veille et al., 1993)] in respective organs.

i. Because it is not possible to measure fetal glomerular filtration rate (GFR) or renal function in utero, inulin clearance measured in preterm and term newborns were collected as a surrogate for fetal GFR. It is worth pointing out that GFR value continues to increase after birth as a result of the drop in renal vascular resistance and increase in renal blood flow (Guignard et al., 1975). Consequently, only measurements taken within 7 days post birth were included in our literature search.

j. Fetal rest of body compartment was back-calculated as fetal weight [based on published fetal volume formula (Abduljalil, Furness et al. 2012) assuming a 1mg/mL density throughout gestation] minus the sum of fetal organ volumes and fetal blood volume [based on the reported average fetoplacental blood volume of 123mL/kg fetal weight during the second and third trimesters (Pasman et al., 2009)].

DMD Fast Forward. Published on June 6, 2017 as DOI: 10.1124/dmd.117.075192
This article has not been copyedited and formatted. The final version may differ from this version.

Table 2: Summary of drug-specific parameters used in the simulations at term (week 40)

Parameter	Drug X	Drug Y
Molecular Weight	236.23[a]	325.8[i]
logP	0.05[b]	3.13[i]
B/P Ratio	1.17[c]	0.66[i]
V_{ss} (L/kg)	0.71[d]	1.1[i]
$f_{u,plasma}$	0.99[e]	0.032[i]
F_a	1.0[f]	0.88[i]
k_a (h^{-1})	1.5[g]	4.0[j]
F_g	0.78[f]	0.58[i]
CL_r (L/h)	18.1[d]	0.085[i]
CL_{iv} (L/h)	45.6[d]	43.0[i]
CL_{PD} (L/h)	1.80[h]	22.7[k]
f_m and f_e	f_m =61%, f_e =39%[d]	$f_{m,3A}$ =92%, $f_e \approx 0\%$[i]
CL_{f0} (L/h)	0.9[h]	0[m]

The above values for drug X and drug Y at term (week 40) were based on the reported didanosine and midazolam PK parameters in the literature, respectively.

a. Extracted from didanosine product monograph (http://monographs.iarc.fr/ENG/Monographs/vol76/mono76-9.pdf).

b. Literature value (Tuntland et al., 1999).

c. Calculated from the reported blood: plasma didanosine AUC ratio (Barry et al., 1993).

d. Predicted by Simcyp® (Version14) based on literature value (Knupp et al., 1991). V_{ss} increased slightly from 0.68 L/kg at week 20 to 0.71 L/kg to week 40.

e. Reported plasma binding of didanosine is <5%. Minimal binding of 1% was assumed for ease of data interpretation.

f. Reported average didanosine absolute bioavailability is 23.5% (Range: 14%-33% [77]) (Knupp et al., 1991). Animal studies indicate that didanosine is rapidly and completely absorbed. Therefore, F_a was assumed to be 1. The reported intravenous non-renal clearance (~30L/h) (Knupp et al., 1991) does not fully explain the first pass effect. F_g of 0.78 was used to recover oral PK.

g. Literature value (Velasque et al., 2007).

h. Irreversible human fetal drug X clearance at term was calculated as the product of fetal didanosine clearance in the macaque fetus [dam weight normalized (Tuntland et al., 1999)] and the average term body weight of 85 kg in human pregnant women (Abduljalil et al., 2012). The reported steady-state fetal:dam didanosine plasma concentration ratio is ~0.5 (Tuntland et al., 1999). Therefore, placental passive diffusion clearance was estimated as 1.8 L/h (**Supplementary Eq.2**), assuming the same F:M AUC ratio holds true for drug X in human maternal-fetal pairs.

i. Reported values of midazolam pregnancy PBPK model (Ke et al., 2012).

j. Estimated from midazolam oral data from term pregnant women (Kanto et al., 1983).

k. Estimated from the reported midazolam umbilical venous plasma concentrations (Kanto et al., 1983; Zhang and Unadkat, 2017).

l. Calculated (Zhang and Unadkat, 2017)

m. Assumed.

Table 3 Drug X clearance values (L/h) used in various scenarios

Drug X	Dosing regimen	τ	CL_{m0}	CL_{PD}	CL_{p0}	CL_{f0}	CL_{MP}	CL_{PM}
Figure 2a,b	week 40, 16.7 mg/h continuous IV infusion	N/A	4.5 vs 45	1.8	0	0	0	0
Figure 2c,d	week 40, 400 mg single oral dose	N/A	4.5 vs 45	1.8	0	0	0	0
Figure 2e,f	week 40, 133.3 mg multiple oral doses	8h	4.5 vs 45	1.8	0	0	0	0
Figure 2g,h	week 40, 400mg multiple oral doses	24h	4.5 vs 45	1.8	0	0	0	0
Figure 4a,b	week 40, 16.7 mg/h continuous IV infusion	N/A	45	1.8 vs 18	0	0	0	0
Figure 4c,d	week 40, 400mg single oral dose	N/A	45	1.8 vs 18	0	0	0	0
Figure 4e,f	week 40, 400mgmultiple oral doses	24h	45	1.8 vs 18	0	0	0	0

Figure 6a	week 40, 400mg single oral dose		N/A	45	1.8	0,0.18,0.90,1.8	0	0	0
Figure 6b						0	0,0.18,0.9,1.8	0	0
Figure 6c						0,0.18,0.9,1.8	0,0.18,0.9,1.8	0	0
Figure 6d						0	0	0,0.18,0.9,1.8	0
Figure 6e						0	0	0	0,0.18,0.9,1.8
Figure 8a, b (Scenario 1)	400mg single oral dose	week 20	N/A	44	0.21	0	0	0	0
		week 40		45	1.8	0	0	0	0
Figure 8c, d (Scenario 2)		week 20		44	0.21	0	0.11	0	0
		week 40		45	1.8	0	0.90	0	0
Figure 8e, f (Scenario 3)		week 20		44	0.21	0	0	0	0.70
		week 40		45	1.8	0	0	0	0.36
Figure 8g, h (Scenario 4)		week 20		44	0.21	0	0.11	0	0.70
		week 40		45	1.8	0	0.90	0	0.36

* CL_{m0}, maternal systemic clearance; CL_{PD}, transplacental passive diffusion clearance; CL_{MP}, placental efflux clearance; CL_{PM}, placental uptake clearance; CL_{p0},placental metabolism; CL_{f0}, fetal metabolism; week, gestational week.

** At 40 weeks, CL_{m0} was set at 45L/h based on the published didanosine clearance value (see **Table S1**; rounded down to the nearest integer**)**. CL_{PD} was extrapolated from the reported didanosine transplacental passive diffusion clearance in pregnant macaques based on body weight (see **Table S1** for detail).

Table 4 Drug Y clearance values (L/h) used in various scenarios

Drug Y	Dosing regimen	τ	CL_{m0}	CL_{PD}	CL_{p0}	CL_{f0}	CL_{MP}	CL_{PM}
Figure 3a,b	week 40, 0.63 mg/h continuous IV infusion	N/A	12 vs 43	22.5	0	0	0	0
Figure 3c,d	week 40, 15mg single oral dose	N/A	12 vs 43	22.5	0	0	0	0
Figure 3e,f	week 40, 2.5 mg multiple oral doses	4h	12 vs 43	22.5	0	0	0	0
Figure 3g,h	week 40, 15mg multiple oral doses	24h	12 vs 43	22.5	0	0	0	0
Figure 5a,b	week 40, 0.63 mg/h continuous IV infusion	N/A	43	2.25 vs 22.5	0	0	0	0
Figure 5c,d	week 40, 15mg single oral dose	N/A	43	2.25 vs 22.5	0	0	0	0

Figure 5e,f	week 40, 15mg multiple oral doses		24h	43	2.25 vs 22.5	0	0	0	0
Figure 7a	week 40, 15mg single oral doses		N/A	43	22.5	0, 2,3,11.3,22,5	0	0	0
Figure 7b						0	0, 2,3,11.3,22,5	0	0
Figure 7c						0, 2,3,11.3,22,5	0, 2,3,11.3,22,5	0	0
Figure 7d						0	0	0, 2,3,11.3,22,5	0
Figure 7e						0	0	0	0, 2,3,11.3,22,5
Figure 9a, b,c (Scenario 1)	400mg single oral dose	week 20	N/A	34.8	2.2	0	0	0	0
		week 40		43	22.5	0	0	0	0
Figure 9c,d,e (Scenario 2)		week 20		34.8	2.2	0	0	0	0
		week 40		64.1	22.5	0	0	0	0
Figure 9e,f,g (Scenario 3)		week 20		34.8	2.2	0	0	0	4.5
		week 40		43	22.5	0	0	0	7.4
Figure 9h,i,j (Scenario 4)		week 20		34.8	2.2	0	0	0	4.5
		week 40		64.1	22.5	0	0	0	7.4

* CL_{m0}, maternal systemic clearance; $CL_{PD.u}$, unbound transplacental passive diffusion clearance; $CL_{MP,u}$, unbound placental efflux clearance; $CL_{PM,u}$, unbound placental uptake clearance; $CL_{p0,u}$, unbound placental metabolism; $CL_{0,u}$, unbound fetal metabolism; week, gestational week.

** At week 20, baseline value CL_{m0} was set at 43L/h based on the published midazolam clinical data at term (Ke et al., 2012), whereas $CL_{PD,u}$ was estimated through sensitivity analysis to match reported fetal UV plasma midazolam drug concentration-time profile (Zhang and Unadkat, 2017). At week 20, CL_{m0} was slightly decreased primarily resulting from more plasma albumin binding.

Table 5 Gestational age-dependent changes in the fetal metabolic (CL_{f0}) and placental efflux (CL_{PM}) clearances of drugs X and Y

Drug	X			Y		
Clearance (L/h)	Gestational age week 20	Gestational age week 40	week 40: week 20 ratio	Gestational age week 20	Gestational age week 40	week 40: week 20 ratio
CL_{PD}*	0.21	1.80	8.6	2.2	22.4	9.
CL_{f0}	0.11 (53% of CL_{PD})	0.90 (50% of CL_{PD})	8.2	0	0	N/A
CL_{PM}**(P-gp mediated)	0.70 † (330% of CL_{PD})	0.36 (20% of CL_{PD})	0.51	7.4 (336% of CL_{PD})	4.5 (20% of CL_{PD})	0.6

* Denotes transplacental passive diffusion clearance after accounting for binding.

** Denotes efflux clearance mediated by P-gp located on the apical side of placenta; assumed to be 20% of CL_{PD} at week 40.

† Back extrapolated based on the assumed 5-fold decrease in placental P-gp expression and the reported 2.6-fold increase in the placenta volume (Abduljalil et al., 2012).

Figure 1

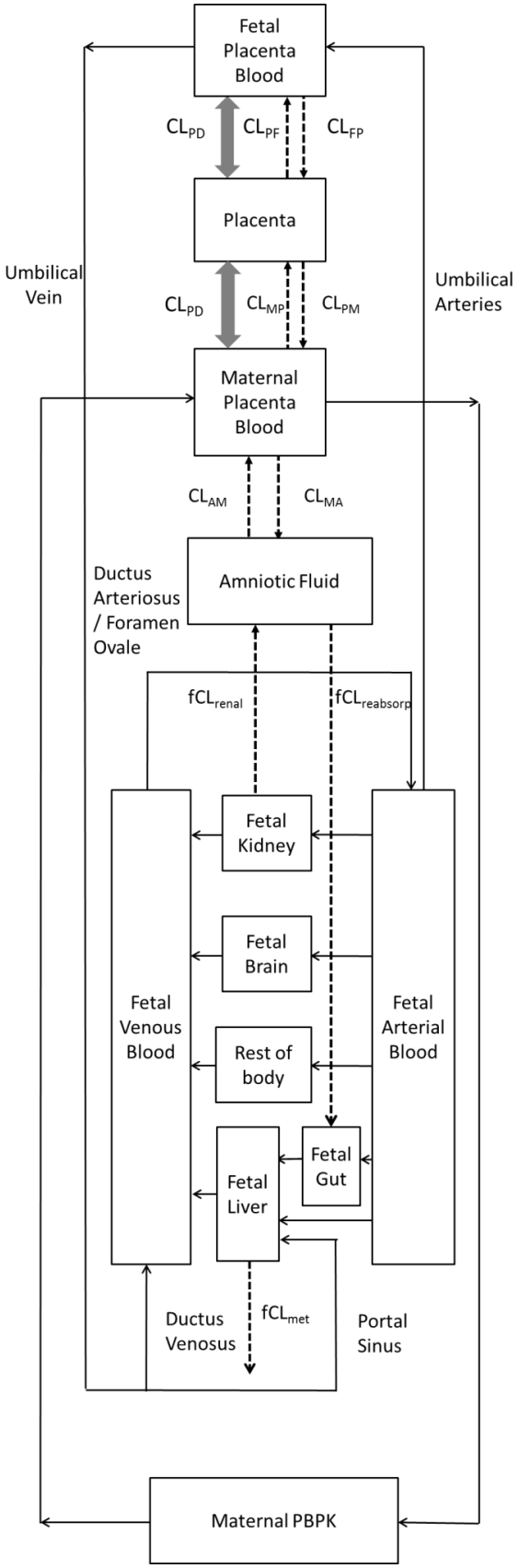
Fetal Placenta Blood
CL_{PD}
CL_{PF}
CL_{FP}
Placenta
Umbilical Vein
CL_{PD}
CL_{MP}
CL_{PM}
Umbilical Arteries
Maternal Placenta Blood
CL_{AM}
CL_{MA}
Ductus Arteriosus / Foramen Ovale
Amniotic Fluid
fCL_{renal}
$fCL_{reabsorp}$
Fetal Kidney
Fetal Brain
Fetal Venous Blood
Fetal Arterial Blood
Rest of body
Fetal Gut
Fetal Liver
Ductus Venosus
fCL_{met}
Portal Sinus
Maternal PBPK

Figure 2

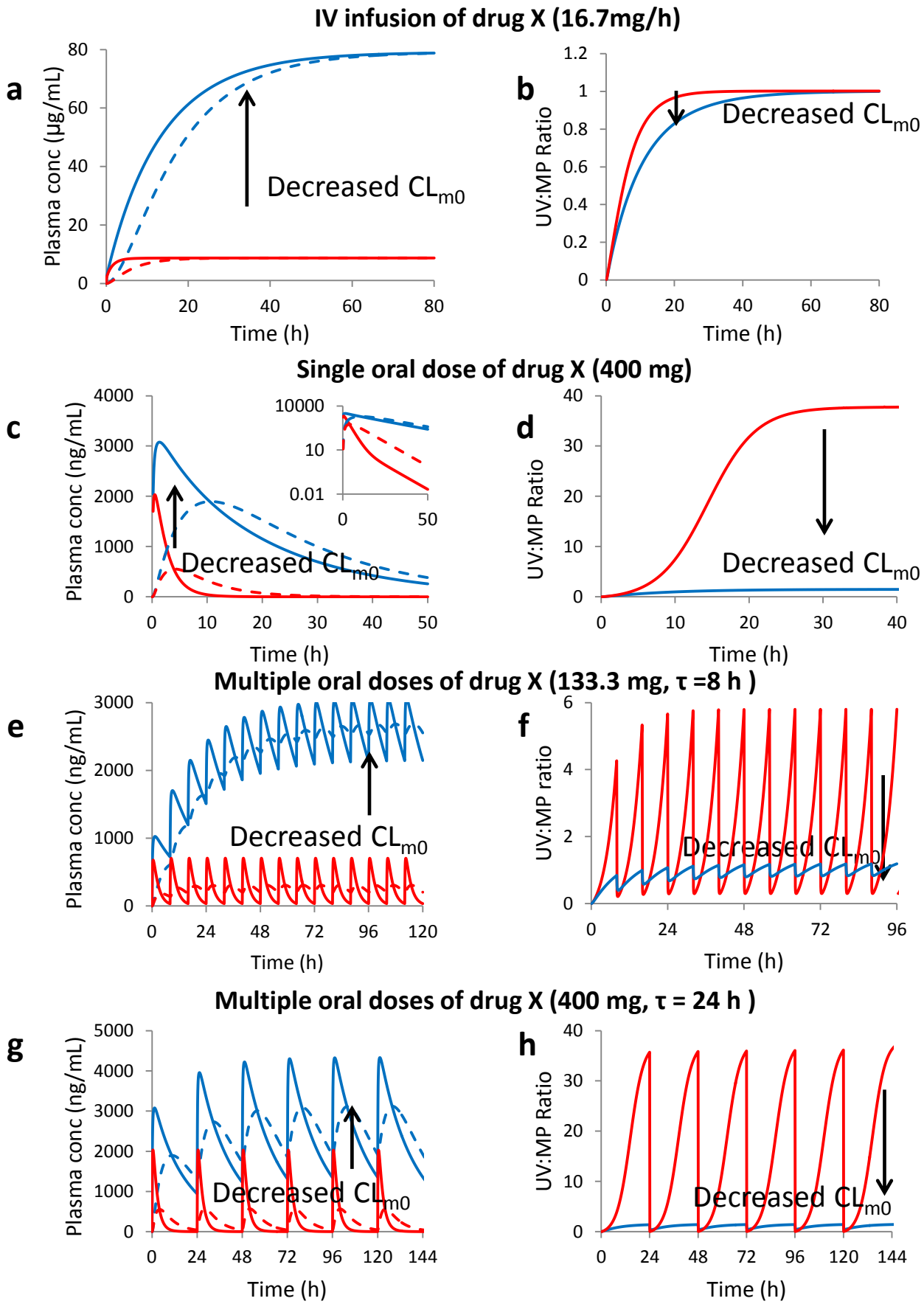
IV infusion of drug X (16.7mg/h)
a
Plasma conc (µg/mL)
Time (h)
Decreased CLm0
b
UV:MP Ratio
Time (h)
Decreased CLm0
Single oral dose of drug X (400 mg)
c
Plasma conc (ng/mL)
Time (h)
Decreased CLm0
d
UV:MP Ratio
Time (h)
Decreased CLm0
Multiple oral doses of drug X (133.3 mg, τ =8 h)
e
Plasma conc (ng/mL)
Time (h)
Decreased CLm0
f
UV:MP ratio
Time (h)
Decreased CLm0
Multiple oral doses of drug X (400 mg, τ = 24 h)
g
Plasma conc (ng/mL)
Time (h)
Decreased CLm0
h
UV:MP Ratio
Time (h)
Decreased CLm0

Figure 3

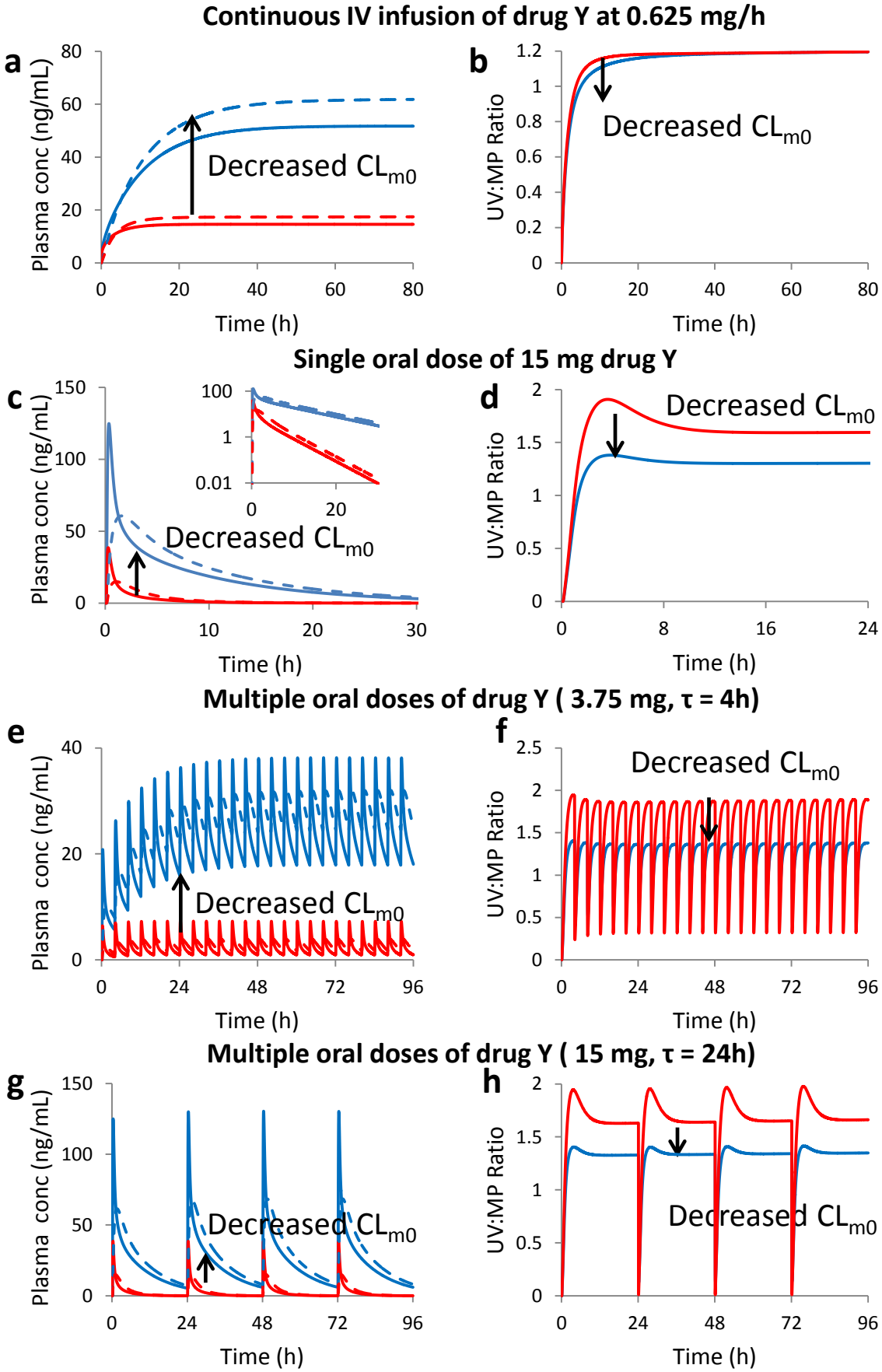
Continuous IV infusion of drug Y at 0.625 mg/h
a
Plasma conc (ng/mL)
Time (h)
Decreased CLm0
b
UV:MP Ratio
Time (h)
Decreased CLm0
Single oral dose of 15 mg drug Y
c
Plasma conc (ng/mL)
Time (h)
Decreased CLm0
d
UV:MP Ratio
Time (h)
Decreased CLm0
Multiple oral doses of drug Y (3.75 mg, τ = 4h)
e
Plasma conc (ng/mL)
Time (h)
Decreased CLm0
f
UV:MP Ratio
Time (h)
Decreased CLm0
Multiple oral doses of drug Y (15 mg, τ = 24h)
g
Plasma conc (ng/mL)
Time (h)
Decreased CLm0
h
UV:MP Ratio
Time (h)
Decreased CLm0

Figure 4

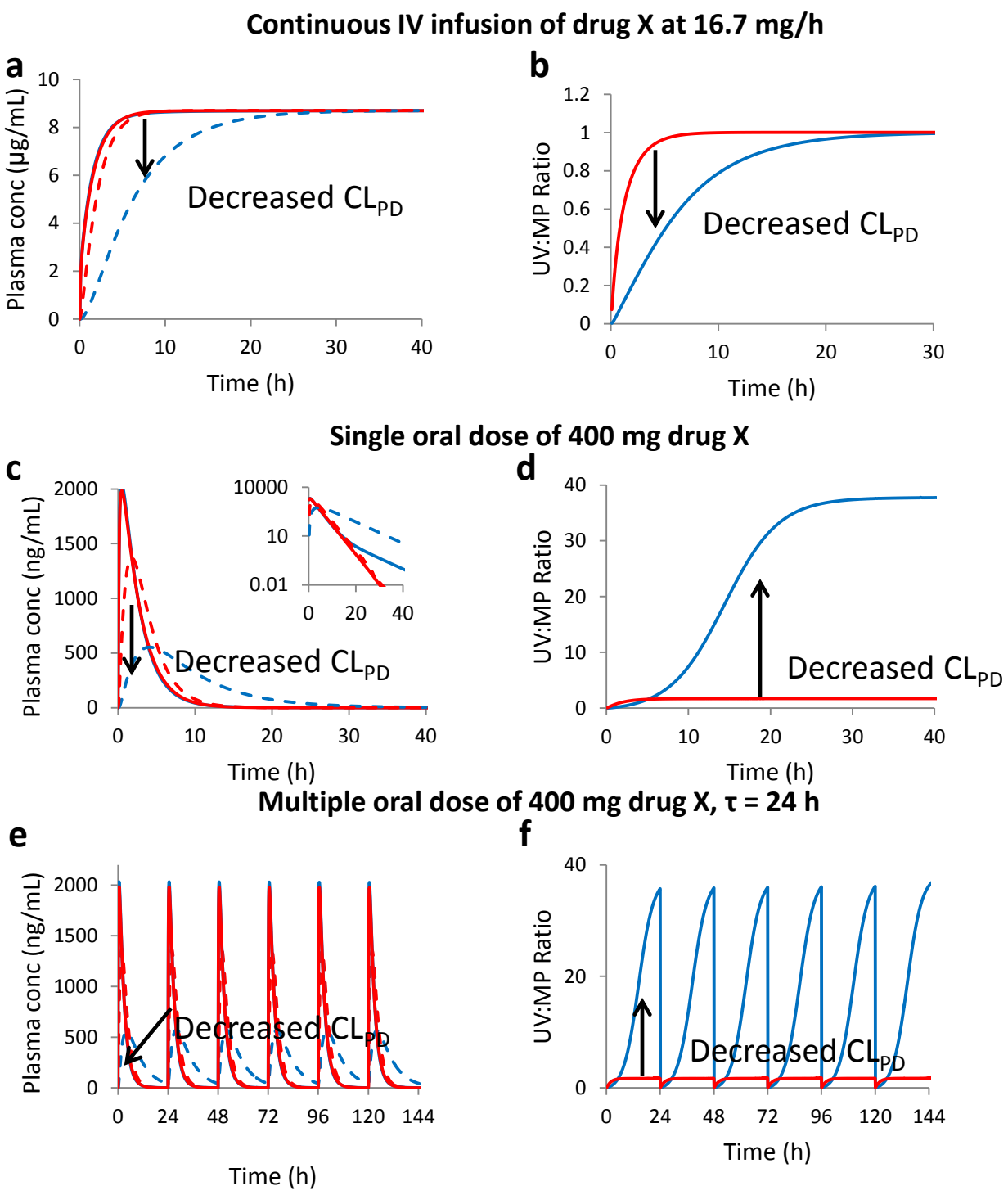
Continuous IV infusion of drug X at 16.7 mg/h
a
Plasma conc (µg/mL)
Time (h)
Decreased CLPD
b
UV:MP Ratio
Time (h)
Decreased CLPD
Single oral dose of 400 mg drug X
c
Plasma conc (ng/mL)
Time (h)
Decreased CLPD
d
UV:MP Ratio
Time (h)
Decreased CLPD
Multiple oral dose of 400 mg drug X, τ = 24 h
e
Plasma conc (ng/mL)
Time (h)
Decreased CLPD
f
UV:MP Ratio
Time (h)
Decreased CLPD

Figure 5

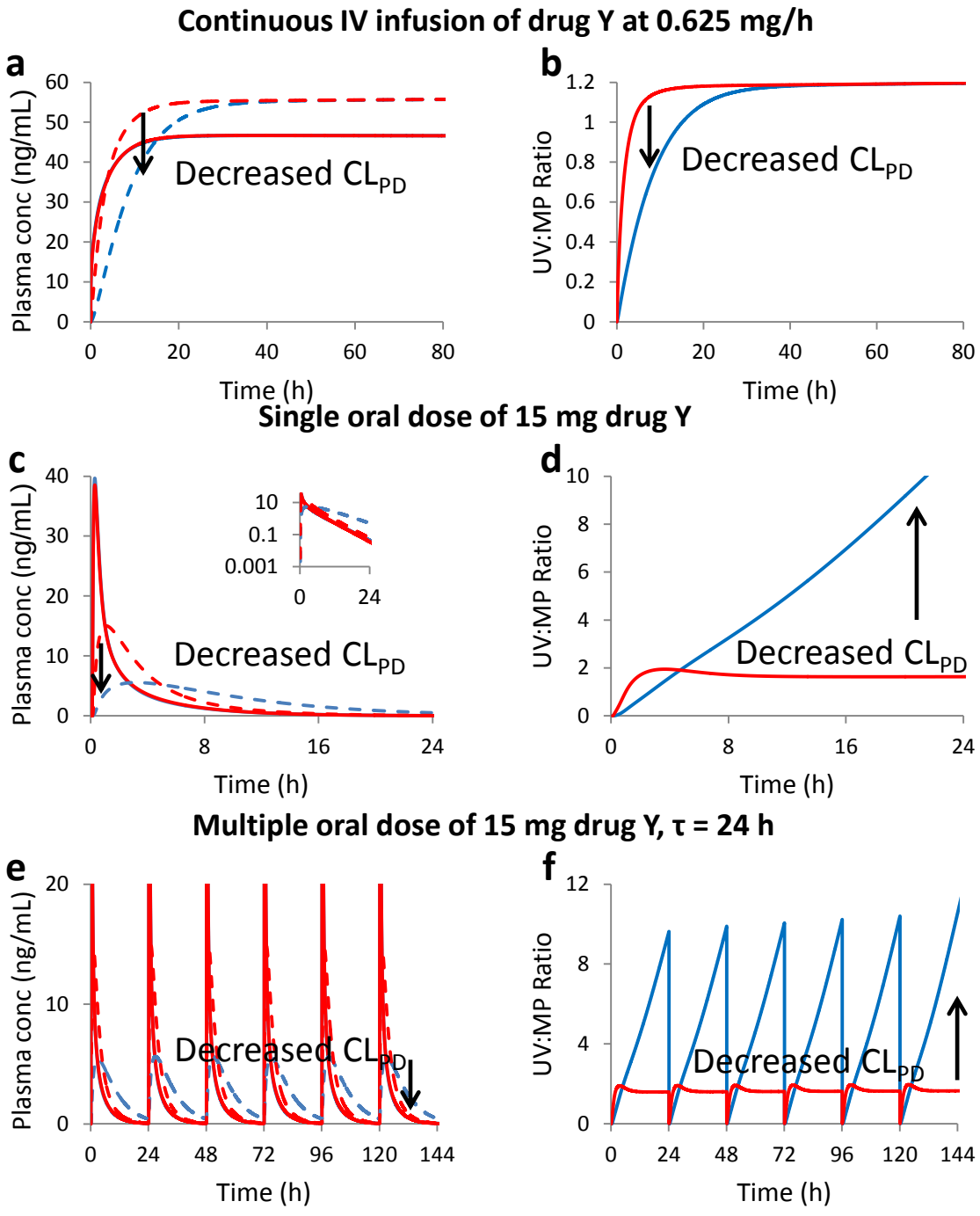
Continuous IV infusion of drug Y at 0.625 mg/h
a
Plasma conc (ng/mL)
Time (h)
Decreased CLPD
b
UV:MP Ratio
Time (h)
Decreased CLPD
Single oral dose of 15 mg drug Y
c
Plasma conc (ng/mL)
Time (h)
Decreased CLPD
d
UV:MP Ratio
Time (h)
Decreased CLPD
Multiple oral dose of 15 mg drug Y, τ = 24 h
e
Plasma conc (ng/mL)
Time (h)
Decreased CLPD
f
UV:MP Ratio
Time (h)
Decreased CLPD

Figure 6

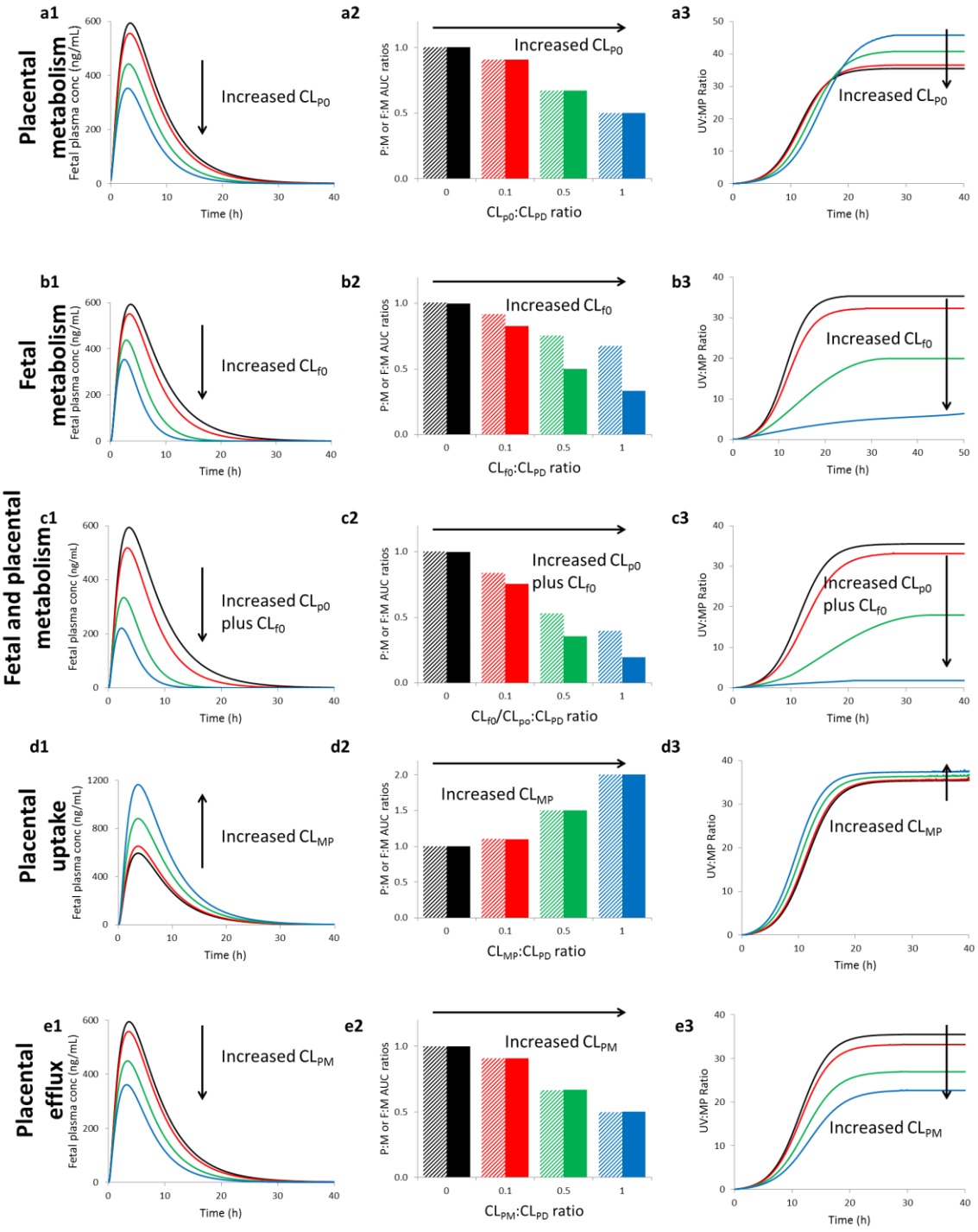
a1
Placental metabolism
Fetal plasma conc (ng/mL)
Increased CL_{P0}
Time (h)
a2
Increased CL_{P0}
P:M or F:M AUC ratios
CL_{p0}:CL_{PD} ratio
a3
Increased CL_{P0}
UV:MP Ratio
Time (h)
b1
Fetal metabolism
Increased CL_{f0}
b2
Increased CL_{f0}
CL_{f0}:CL_{PD} ratio
b3
Increased CL_{f0}
c1
Fetal and placental metabolism
Increased CL_{p0} plus CL_{f0}
c2
Increased CL_{p0} plus CL_{f0}
CL_{f0}/CL_{po}:CL_{PD} ratio
c3
Increased CL_{p0} plus CL_{f0}
d1
Placental uptake
Increased CL_{MP}
d2
Increased CL_{MP}
CL_{MP}:CL_{PD} ratio
d3
Increased CL_{MP}
e1
Placental efflux
Increased CL_{PM}
e2
Increased CL_{PM}
CL_{PM}:CL_{PD} ratio
e3
Increased CL_{PM}

Figure 7

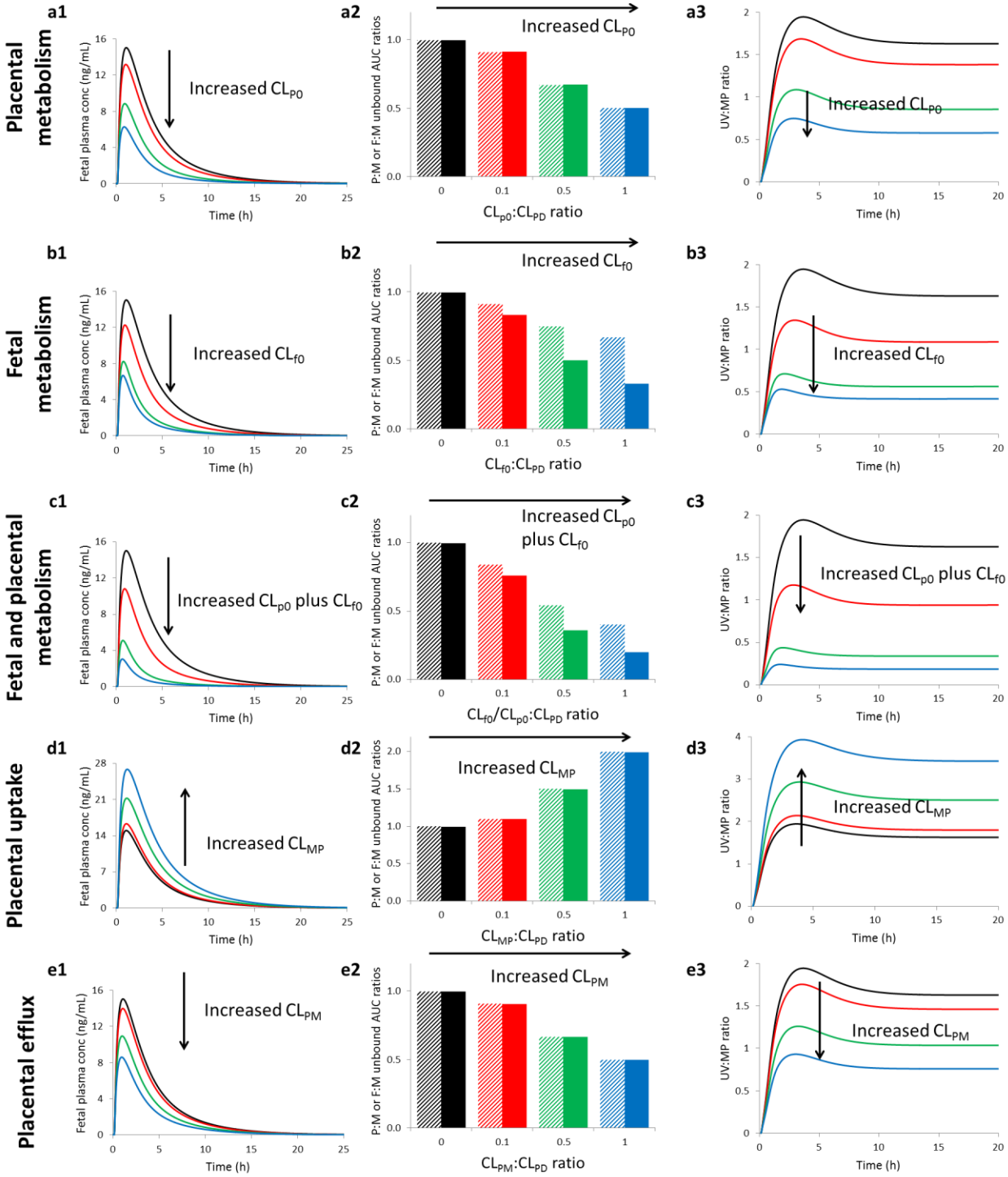
Placental metabolism
a1
Fetal plasma conc (ng/mL)
Increased CL_{P0}
Time (h)
a2
Increased CL_{P0}
P:M or F:M unbound AUC ratios
CL_{p0}:CL_{PD} ratio
a3
UV:MP ratio
Increased CL_{P0}
Time (h)
Fetal metabolism
b1
Increased CL_{f0}
b2
Increased CL_{f0}
CL_{f0}:CL_{PD} ratio
b3
Increased CL_{f0}
Fetal and placental metabolism
c1
Increased CL_{p0} plus CL_{f0}
c2
Increased CL_{p0} plus CL_{f0}
CL_{f0}/CL_{p0}:CL_{PD} ratio
c3
Increased CL_{p0} plus CL_{f0}
Placental uptake
d1
Increased CL_{MP}
d2
Increased CL_{MP}
CL_{MP}:CL_{PD} ratio
d3
Increased CL_{MP}
Placental efflux
e1
Increased CL_{PM}
e2
Increased CL_{PM}
CL_{PM}:CL_{PD} ratio
e3
Increased CL_{PM}

Figure 8

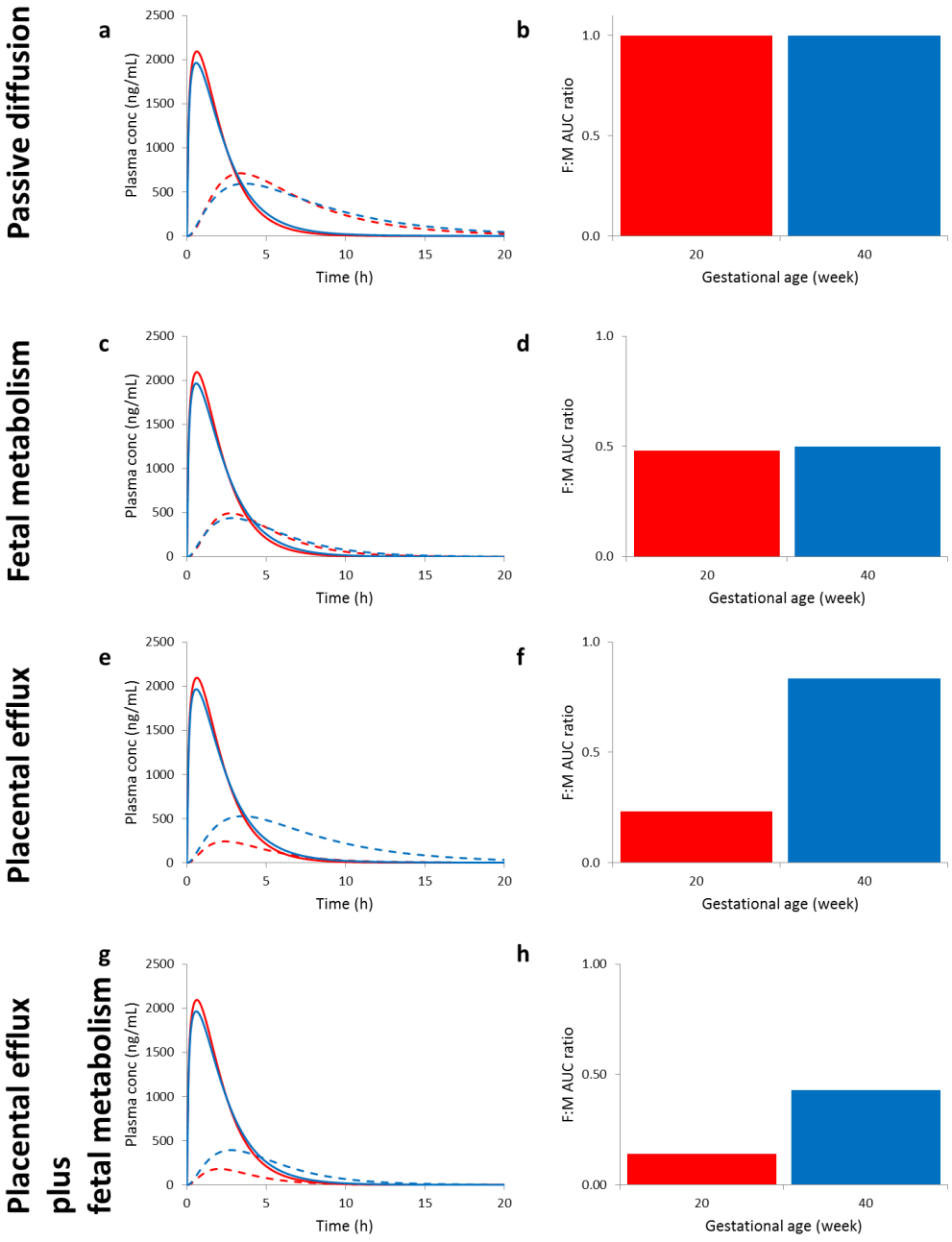
Passive diffusion
Fetal metabolism
Placental efflux
Placental efflux plus fetal metabolism
a
b
c
d
e
f
g
h
Plasma conc (ng/mL)
Time (h)
F:M AUC ratio
Gestational age (week)

Figure 9

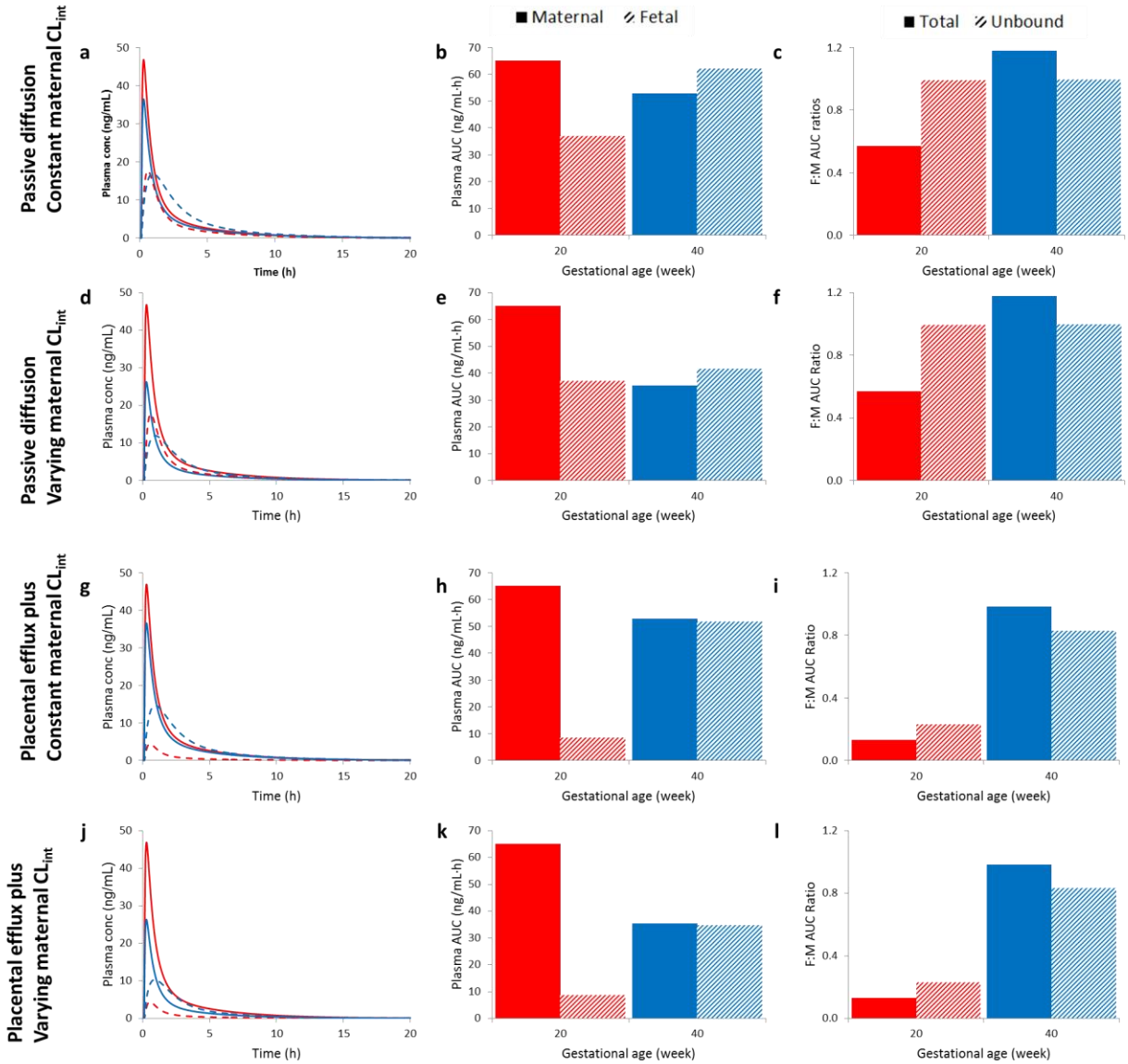
Passive diffusion
Constant maternal CL_{int}
a
Plasma conc (ng/mL)
Time (h)
b
Maternal
Fetal
Plasma AUC (ng/mL·h)
Gestational age (week)
c
Total
Unbound
F:M AUC ratios
Gestational age (week)
Passive diffusion
Varying maternal CL_{int}
d
Plasma conc (ng/mL)
Time (h)
e
Plasma AUC (ng/mL·h)
Gestational age (week)
f
F:M AUC Ratio
Gestational age (week)
Placental efflux plus
Constant maternal CL_{int}
g
Plasma conc (ng/mL)
Time (h)
h
Plasma AUC (ng/mL·h)
Gestational age (week)
i
F:M AUC Ratio
Gestational age (week)
Placental efflux plus
Varying maternal CL_{int}
j
Plasma conc (ng/mL)
Time (h)
k
Plasma AUC (ng/mL·h)
Gestational age (week)
l
F:M AUC Ratio
Gestational age (week)